ISSN: 1650-1888
TRITA: IIP-13-01

OSCAR ANDERSSON Process planning of resistance spot welding

KTH 2013

www.kth.se

Process planning of resistance spot welding

OSCAR ANDERSSON

Licentiate Thesis in Production Engineering
Stockholm, Sweden 2013

KTH Industrial Engineering
and Management

Abstract

Manufacturing engineering in general has experienced an increased demand of process planning in order to optimize processes to reduce costs, environmental impact and increase time efficiency. Resistance spot welding (RSW) is a common and large-scale joining method in several manufacturing industries indicating significant potentials of efficient process planning.

The goal of this thesis is to establish new knowledge for updated and improved process planning of RSW in industrial applications. The goal is expressed by two research questions targeting the issues of process variations and potential of numerical methods of the RSW process. The research questions are expressed in terms of weld size, which is the main interest in RSW process planning.

As any large-scale manufacturing process, RSW involves variations in results – the weld size is known to vary, both as a result of intentional dependent parameters such as process parameters and as a result of unintentional variations in welding conditions. A series of physical and numerical analysis have been performed in order to gain knowledge of such variations.

The unintentional variations, which result in varying weld sizes in apparently identical conditions, were analyzed through both controlled laboratory welding and welding in industrial production environments. The results of the analysis showed the magnitude of standard deviations in both environments and the distribution of weld sizes. The analysis showed that common standard deviations in controlled laboratories and industrial production are approximately 0.3 mm and 0.9 mm, respectively and that weld sizes are distributed showed promising fit to both Normal and Weibull distributions.

The intentional variations of weld sizes due to process parameters, which is the most important aspect of RSW process planning, have traditionally been analyzed through physical testing. In the present thesis two numerical methods were evaluated; regression analysis and FE simulations. For the regression analysis several models were generated and showed a standard deviation of residuals between model and physical results of 0.5 mm. For the FE simulations, material models for the RSW were generated and the simulations showed a standard deviation compared to physical testing of 0.68 mm. In conclusion, the present thesis presents results, which help quantify variations in weld sizes and present the capability of numerical methods of the RSW process.

Acknowledgement

This thesis is the result of my research at the department of production engineering, Royal Institute of Technology, Stockholm within the project SpotLight between January 2010 and December 2012. The project was funded by VINNOVA and the project partners; Gestamp Hardtech, Royal Institute of Technology, SAPA, Scania, SSAB, Swerea IVF, Swerea KIMAB, Volvo Car Group, Volvo Trucks and University West.

My gratitude goes to my supervisor Professor Arne Melander for continuous guidance and support throughout my work. Joel Lundgren, Gert Larsson and Lars-Ola Larsson at Volvo Car Group have all helped my work with their general knowledge in resistance spot welding and industrial implementations. I would also like to thank Martin Olsson and Benny Andersson at Volvo Car Group for their help in conducting experiments. Acknowledgement is also due to Johannes Gårdstam at Swerea KIMAB for his guidance in welding simulation.

Finally, a special thank you is due to my friends and family, who have supported me during my research.

Oscar Andersson

Table of contents

Nomenclature

B	Flow stress parameter	[-]
C	Thermal expansion matrix	[T^{-1}]
s	Sheet thickness	[m]
D	Stiffness matrix	[Pa]
H	Enthalpy	[J]
I	Current	[A]
J	Current density	[A m^{-2}]
k	Thermal conductivity	[$W \cdot m^{-1} \cdot K^{-1}$]
K	Effective thermal conductivity	[$W \cdot m^{-1} \cdot K^{-1}$]
n	Flow stress parameter	[-]
Q	Heat	[W]
q	Pressure	[Pa]
r	Radial direction	[-]
R	Electrical resistance	[Ω]
t	Time	[s]
T	Temperature	[K]
u	Displacement	[m]
V	Voltage	[V]
X	Input matrix for regression model	
Y	Results matrix for regression model	
z	z-direction	[-]
ε	Strain	[-]
ε_{pl}	Plastic strain	[-]
ρ	Density	[$kg \cdot m^{-3}$]

κ	Electrical conductivity	[S m^{-1}]
σ	Stress	[Pa]
σ_Y	Yield stress	[Pa]
Θ	Circumferential direction	[-]

1 Introduction

Industries and consumers in general are subject to pressure to reduce greenhouse gas emissions, caused by their manufacturing and the use of their products, to reduce the effects of global warming [1] The automotive industry – one of the dominant sources of greenhouse emissions [2] - has answered to this pressure mainly by reducing fuel consumption by producing more fuel efficient engines, reducing the weight of products [3] and introducing alternative fuel engines [4].

The reduction in weight of vehicles is made possible by innovative designs and use of materials of high strength to weight ratios, such as high-strength steels, aluminum or composite materials [5]. These solutions are associated with challenges in manufacturing due to the novelty and complexity of the components and materials.

Joining technology is an integral part of modern manufacturing and joining properties are an important aspect of product properties in general. The increased complexity of vehicle products has also resulted in challenges for joining technologies.

Process planning is a key element of any successful process in manufacturing engineering. In resistance stop welding and the present thesis, process planning is mainly focused on optimization of process parameters with regard to product properties, process time efficiency and cost of the process. The process planning progress is illustrated in Figure 1, where a given set of weld materials, weld equipment and applications can be welded with a set of weld process parameters. These parameters shall be optimized in order to give sufficient weld results.

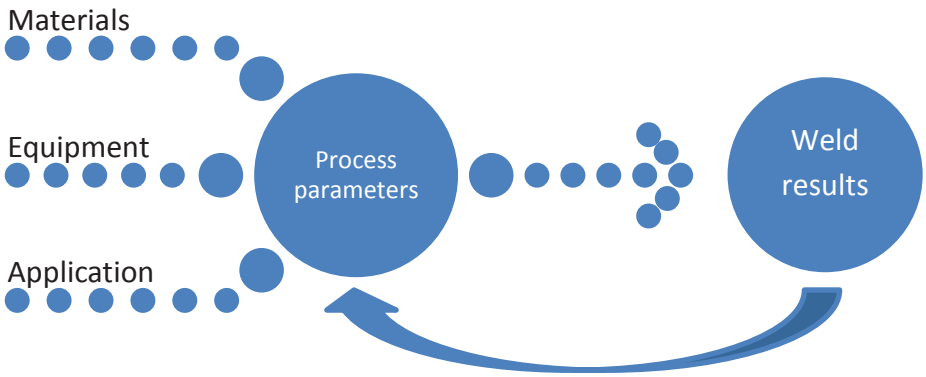

Figure 1 Process planning in RSW applications.

1.1 Background

In the transportation industry, and the automotive industry in particular, resistance spot welding (RSW) has for decades been the main joining technology. The method's low cost, high reliability, high time efficiency, high accessibility and high ability for robot automatization, compared to other joining methods, make it ideal for automotive production. A typical modern automobile contains around 3000 – 5000 resistance spot welds, while other joining methods, such as laser welding, arc welding or mechanical fastenings is used in a much more limited scale. A typical resistance spot weld is shown in Figure 2. [6]

The large scale of RSW in manufacturing makes the method's results highly important for product properties, including critical properties such as vehicle safety, crashworthiness and fuel efficiency [6]. In order to ensure robustness in RSW applications, variations of process results should be minimized. In order to be minimized, the process variations must be correctly understood and predicted. An important step for understanding and predicting process variations is through process planning.

Figure 2 Section cut of resistance spot weld between two sheets.

To measure weld quality and process robustness of RSW, the main measurements are weld nugget size (the lateral size of the solidified joint zone) and the occurrence of weld expulsion. Expulsion is the phenomenon which occurs when molten metal is ejected from the weld. While, the two measurements do not fully measure all aspects of weld quality, they indicate several important factors and are relatively easy to attain.

In general, process planning may include a broad range of analysis and measures. Regarding RSW, however, process planning is focused on process parameters. By understanding the effect of process parameters and their optimization, the RSW process' result properties and robustness can be improved.

The lack of accurate large scale non-destructive test (NDT) methods for RSW increases the importance of process planning for RSW applications [7]. Therefore, the predictive capability of process planning tools must be sufficient in order to accurately model production scale RSW processes.

Optimization of RSW process parameters have traditionally been performed through empirical experimental testing in laboratory environments. Such physical testing is accurate and reliable but it also has its downsides. Physical testing always involves material supply, welding equipment and operator skills, all of which are costly and critical for the results. In many fields of research, numerical modeling has been used partly or fully as a replacement for experimental testing. Numerical models can be used as an effective tool in virtual process planning.

In general joining research, promising results of numerical models have been published. Several methods, such as simpler regression models [8] or more

advanced FE simulations [9] have been used to model welding processes accurately. Also, specifically regarding RSW, numerical methods have been shown in literature but a large-scale use of simulations for process planning is yet to be presented. A more detailed review of the development of numerical models is presented in this thesis.

In this thesis, virtual process planning of RSW is treated through several methods. Studies showing the variations of RSW results as well as the capability of numerical methods for large scale implementation are presented. Such variations have been previously reported [10], [11] but have not been quantified. The variations are studied through repeated welding of apparently identical welds and destructively tested and evaluated. The numerical methods are studied through development of regression models and FE simulations. The results of the numerical models are compared to physical tests, which are destructively tested and evaluated. A more detailed introduction to the appended papers is made in chapter 1.5.

1.2 Outline to the thesis

Following this introductory chapter, a presentation of the theoretical background of the subject is made in chapter 2. The theoretical background includes the physical phenomena behind the RSW process, evaluation methods of weld quality and theories regarding RSW simulations. The background chapter is followed by a summary of the results achieved from a number of appended papers. Lastly, the thesis includes a discussion regarding the results and proposes future research in the field.

1.3 Research questions

The present thesis aims to answer two research questions. Both treat different aspects of process planning of RSW and aim to improve the properties and robustness of RSW applications. Together they form a broad approach to virtual process planning of RSW, and tackle significant issues for improvement of RSW quality and process robustness.

The first question regards variations of RSW properties and is stated as follows.

- **I: How large are variations of resistance spot weld sizes?**

The second question regards improvements of process planning in terms of experimental testing.

- **II: How accurately can numerical models predict resistance spot weld sizes?**

1.4 Research methodology

To be able to answer the research questions a research framework has been used as methodology. The theoretical background for the framework is obtained from research done in several fields, ranging from statistics, geometry distortions, material modeling and simulation methods. Scientific papers, journals and book have been studied to create the theoretical base of the thesis. The results were based on experimental work combined with statistical and numerical models.

1.5 Introduction to the papers

Appended are five papers, which treat the subject of process planning of RSW and include the results of the thesis. The papers include several aspects of process planning and the results can be implemented in different stages of process planning.

The papers include studies on statistical analysis of RSW result variations, regression models for RSW result prediction and simulation methods for RSW result prediction. Each of the papers is briefly introduced below and described how they answer the research questions introduced earlier.

1.5.1 PAPER A: Statistical Analysis of Variations of Resistance Spot Weld Nugget Sizes

In *Proceedings of the 64th* IIW Annual Assembly *& International Conference,* 2011.

As an initial study of process planning, the variations of RSW results were analyzed. The first paper includes experimental RSW results from a laboratory environment, where apparently identical welding was performed repeatedly. A large amount of weld size data was recorded and the variations in weld sizes were measured and analyzed. The experiments were done to quantify the variations of RSW results in apparently identical welding conditions, due to natural variations.

The effects of electrode tip dressing, welding current, electrode force and contact resistance on weld nugget size and expulsion occurrence, respectively, were analyzed.

Furthermore, statistical modeling to describe the result variations was performed. Such a statistical model, in form of a distribution function, can further provide understanding of the variations of the process.

The paper provides analyses of causes of variations and a statistical model for describing variations and is intended to answer research question I.

1.5.2 PAPER B: Statistical Analysis of Variations in Resistance Spot Weld Results in Laboratory and Production Environment

In *Proceedings of the 5th Swedish Production Symposium*, 2012.

The second paper is a continuation of the first paper. Here, RSW results from laboratory as well as production environments were included.

Further measurement and analysis of weld results were presented. The paper aimed to show the possible differences in results between the controlled, ideal conditions of the laboratory and the production environment where the RSW process is affected by several other aspects of manufacturing variations and more complex geometries. The paper gives a more detailed answer to research question I.

1.5.3 PAPER C: General Regression Models for Prediction of Spot Weld Sizes

In *Proceedings of IIW International Congress Advances in Welding Technology & Science for Construction, Energy and Transportation Systems,* 2011

The third paper used experimental welding results from a broad range of material configurations as base for regression models used for RSW process planning. Several regression models were generated and evaluated through systematic statistical methods, as an answer to research question II. The regression models were evaluated in terms of requirements on input data and ability for industrial implementation as well as prediction capability.

The models show the effect of process parameters and material configuration on RSW results. The models can thus be used for parameter optimization as well as process robustness studies.

1.5.4 PAPER D: Verification of the Capability of Resistance Spot Welding Simulation

In *Proceedings of the Sheet Metal Welding Conference XV*, 2012.

The fourth paper includes comprehensive physical verification of RSW simulations. Extensive material testing is performed in a laboratory environment and destructively tested. The experimental results are compared to simulation results.

Material modeling is a critical aspect of welding simulations due to multi-physical nature of the process. Thermal, mechanical, electrical and metallurgical effects must be taken into account for accurate modeling. A complete material model for RSW simulations is presented and discussed. A simulation method for prediction of weld size and expulsion occurrence is presented and evaluated.

The paper implements new material models in an extensive range of simulations. The results of the paper can be used as an evaluation of the capability of simulations as a tool for process planning of RSW and an answer to research question II.

1.5.5 PAPER E Verification of the Capability of Resistance Spot Welding Simulation for automotive process planning

Submitted to *Welding Journal*, 2012

The fifth paper is a continuation of the fourth. The material range for verification has been expanded to include six materials of varying strength and material models have been generated for all materials. Furthermore, a more detailed analysis of expulsion has been performed in the virtual process planning environment.

The paper aims to further show the capabilities of simulations of RSW and works as a more general answer to research question II.

2 Theoretical background of the resistance spot welding process

In order to form a framework of the thesis, the RSW process is presented and described in the following chapter.

Resistance spot welding (RSW) is a type of resistance welding, which is characterized by its discrete areas of joining – known as spot welds. Resistance welding, unlike arc welding, is a metal joining method where the materials are joined by use of electrical resistance rather than an electric arc.

The principle behind the joining method is to pass a current through two or more sheets as they are clamped together by an electrode pair. Furthermore, the history, advantages, disadvantages and common applications of spot welding are described in the following chapters.

2.1 History of resistance spot welding

RSW is considered to be invented in the 1880s by Elihu Thomson, when he discovered the principle of joining metals by melting through resistance heating [12]. The RSW processes in use today are based on the same basic principle.

Today, the main application of RSW is in the automotive industry. However, in other products such as in the aerospace industry, appliances, furniture and small scale circuit elements are joined using RSW. [13]

2.2 Physical phenomena in resistance spot welding

As the current is passing through the sheets, the resistances of the circuit cause generation of heat energy. The heat energy (Q) is a function of the current (I), resistance (R) and time (t) as defined by Joule's law, see Equation (**1** below.

$$Q = I^2Rt \tag{1}$$

The heat generation rises the temperature of the materials above the melting point mainly due to surface resistances between the sheets. After the metal sheets have molten the current is stopped and no further heat is generated. The temperature

will decrease again and the joined sheets form a solid nugget, joining the sheets. The outline of the spot welding process is illustrated in Figure 3.

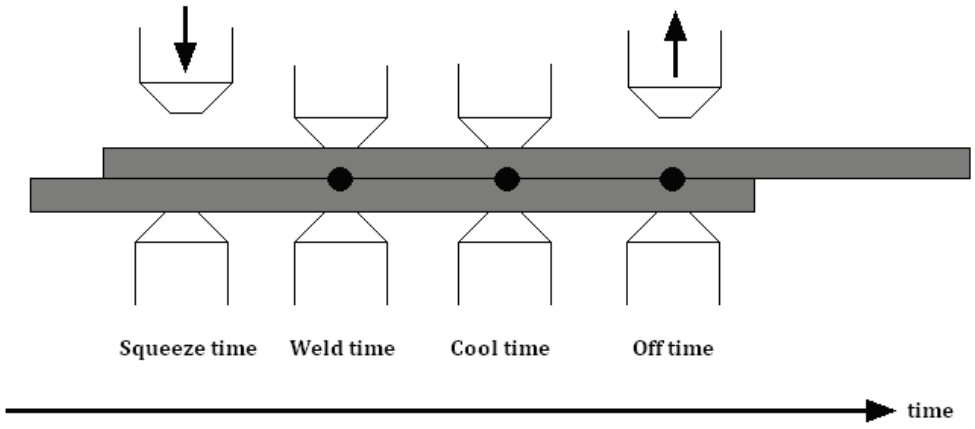

Figure 3 The RSW process timeline.

2.2.1 Thermo-electrical processes of resistance spot welding

An integral part of the resistance spot welding is the thermo-electrical processes which cause the heat generation of the welding. In the following chapters various aspects of the thermo-electrical processes are described.

The heat generated due to the electrical current is defined through Joule's law, equation 1. The resistances, and thus heat generation, of the circuit are located at four major sources, see Figure 4: Typical values of resistances of materials used in RSW can be seen in Figure 5.

- The resistance of the electrodes (1, 7).
- The contact resistance between the electrodes and the sheets (2, 6).
- The bulk resistance of the sheets (3, 5).
- The contact resistance between the sheets (4).

For stack-ups with more than two sheets, bulk resistances and contact resistances are added accordingly.

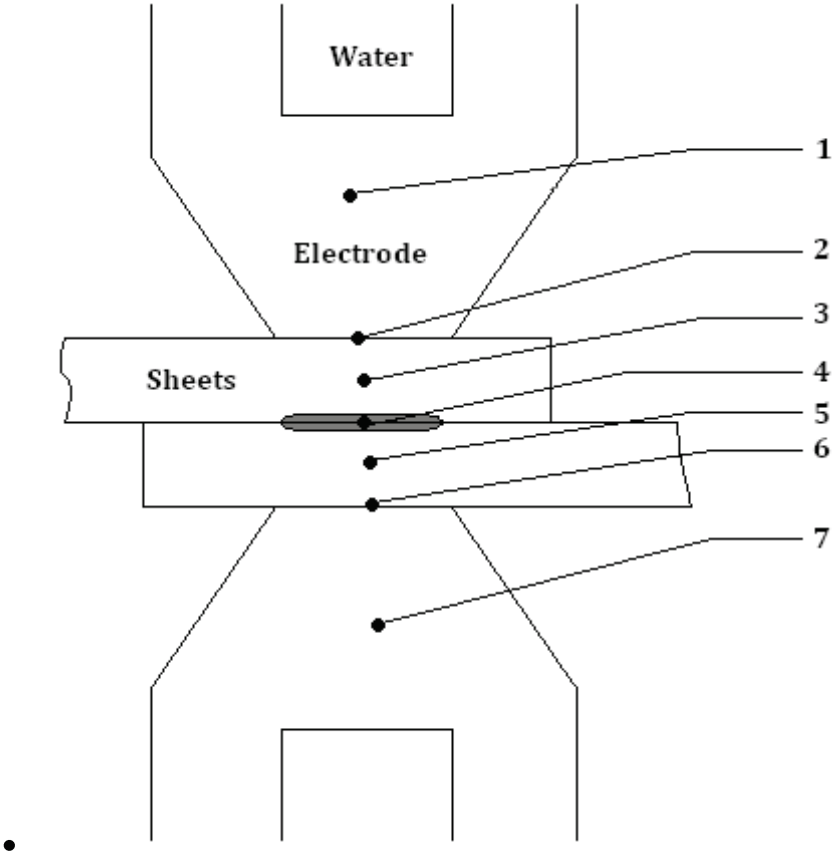

Figure 4 Cross-section of spot weld process and electrical resistances (1-7)

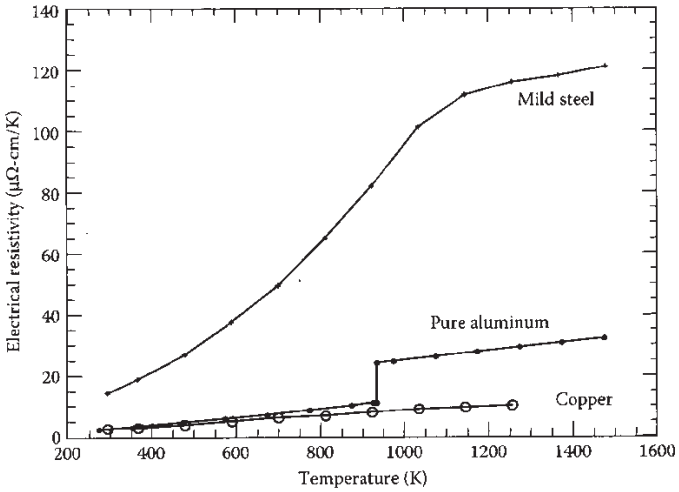

Figure 5 Electrical resistivity of RSW materials. [6]

Since the resistances are connected in a series electrical circuit they will all retard current flow. However, the resistance is a highly temperature dependent variable and will change significantly during the weld process. It can be noted that the resistivity of both aluminum and steel is larger than that of copper of the electrodes. Thus, the heat generated in the work piece is greater than that in the electrodes, which enables welding. This also explains the difficulties to weld aluminum sheets compared to steel, due to the smaller heat generation. However, the contact resistances between the materials are significantly larger and thus, determine the heat generation more, than the bulk resistances of the materials. [6]

To assure electrode contact with the work piece, the electrodes are clamped to the sheets with a mechanical force. The electrodes are most commonly made of a copper alloy. When the electrodes and work piece are in full contact, the electrodes are charged and high amperage current is flowing through the circuit. After the current flow stops the electrodes are squeezing the sheets during a further period, called cool time, to improve controlled nugget formation. The outline of the spot welding process is illustrated in Figure 3. The influence and effect of the input parameters are described in chapter 2.3

For non-constant current or resistance, which is often the case in RSW, the expression in Equation 1 must be integrated to find the correct heat energy. The formula gives a basic understanding of the circuit but is not detailed enough for full understanding. Firstly, in resistance spot welding the local heat generation at each resistance is of more interest than the total heat energy of Joule's law. Secondly, the heating rate is a more indicative parameter of weld development than total heat energy since it has a significant effect on the microstructures of the weld.

Although the Joule effect is the most prominent thermo-electrical effect in resistance spot welding in terms of weld generation, other electro-thermal effects do take place. The Peltier effect, Seebeck effect and Thomson effect all take place during RSW [14] but have a minor effect on weld size and are not treated in detail in the present thesis.

All metals involved in the resistance spot welding process increases in electrical resistance with temperature. Steel is very sensitive to temperature changes, the difference between steel and copper explain the excessive heat in the steel sheets compared to the heat in the electrodes. In addition, the electrodes are water-cooled which decreases their temperature increase, and resistance, further.

Another electrical phenomenon that must be taken into account is shunting currents. Such currents occur when a weld is made in close relation to previously made welds. The adjacent welds create a current path which distorts the intended welding by lowering the effective welding current or current density.

2.2.2 Thermal parameters of resistance spot welding

To create a good weld it is crucial to maintain a low temperature in the electrodes. It will also help in maintaining electrode life. If the electrodes are sufficiently cooled the heat will dissipate effectively through the electrodes due to the high conductivity of copper.

Another important phenomenon observed during welding is thermal expansion. Figure below shows the coefficient of thermal expansion for copper, steel and aluminum at different temperatures. The figure shows the drastic difference between steel and aluminum, which explains the different behavior of the materials during welding.

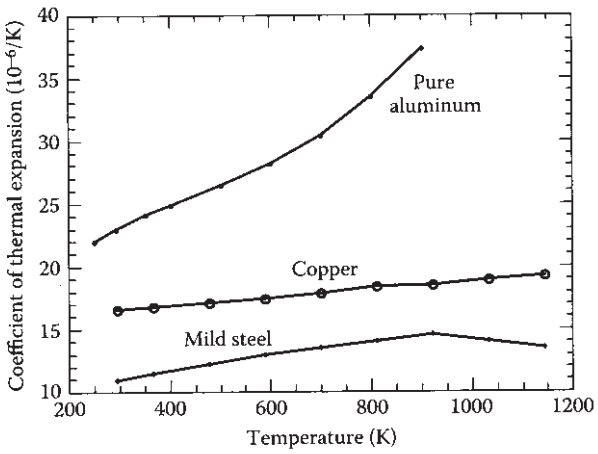

Figure 6 Coefficient of thermal expansion for RSW materials. [6]

The thermal expansion is also the reason why electrode displacement can be used as a parameter for welding monitoring. Heat gain in the nugget will expand the material and try to push the electrodes apart while heat loss works in opposite.

2.3 Resistance spot welding parameters

The resistance spot welding process can be described by a number of parameters, some of which are mentioned above. The weld process can be described by a time-

current-force figure as shown below. In the following chapter each of the machine parameters and their impact on the spot weld is discussed.

2.3.1 Weld current

The welding current is the most effective and common parameter to influence welding result of a given material configuration. A too low current will not provide sufficient heat to create a nugget while a too high current will result in expulsion and even temperatures above the boiling point. Expulsion decreases the nugget size and may also defect surrounding equipment and parts. If the boiling point is reached, there is higher risk for porosity in the finished weld. Another result of too high currents is too large indentations in the metal surface. The current level also affects the distortion of the base metal and the size of the heat affected zone (HAZ). Common welding current amplitude lie in the range of 5kA -10kA depending on sheet configuration, other process parameters and weld requirements. [6]

2.3.2 Weld time

As Joule's law, Equation 1, suggests, the welding time is of importance when calculating heat generation and resulting weld formation. Traditionally, as AC was used, the weld time was measured in periods. As the use of DC has increased, the weld time is now more commonly measured in milliseconds, see Chapter 2.4.1.

As with weld current level a too short weld time will not generate sufficient heat to form a weld a too short weld time may lead to over-heating or expulsion.

In production, there is a need to keep manufacturing times as low as possible to keep costs low. Thus, a shorter weld time is desirable and is more likely to be compensated by higher weld current to give adequate results. In production, typical traditional weld times range between 200 - 700 ms depending on material configuration, other process parameters and weld requirements.

2.3.3 Electrode force

In order to assure contact between the electrodes and the sheets during the entire weld process, the electrodes are clamped to the work piece. The force magnitude is another variable which will affect the outcome of the weld. If the force is too big, the electrical resistance will decrease at the contact surfaces and decreasing heat generation and not melting enough material. It may also cause conduction heat away from the weld area, which is undesirable for nugget formation. Furthermore, too high forces may cause damage to the work piece or excessive deformations.

The surface deformations are especially important in areas where visual quality is of high importance. Examples of such areas may be outer sides of car bodies.

On the other hand, a too low force will increase the risk of geometrical instability of the welding process and excessive heat generation. In other words, the risk for expulsion is increased with a lower force.

Typical electrode forces in automotive manufacturing range between 3 - 6 kN depending on sheet material and thickness. Many conventional modern weld guns are capable of applying weld forces up to 5 kN, while higher forces may require stronger guns or custom modification of weld guns.

2.3.4 Electrode geometry

In production, the shape and size of the electrodes have an effect on the weld outcome. The geometry of a different electrode geometries are shown in Figure 7. The most important parameter in the electrode geometry is the contact area between the electrode and the metal sheet. As a general rule the diameter of the electrode tip should be approximately equal to $5\ \overline{d}$, where d is the thickness of the sheet [6]. The contact will affect both the contact pressure and the current density of the weld. In optimization of weld parameters, it may be ideal to use different electrodes on each side of the stack-up.

The tip curvature of the electrode is a measure against the degradation of the electrode tip. As the electrode degrades the initial curvature will deform into a flat surface. An initially flat surface would cause a concave tip after continuous welding.

The most commonly used electrode geometries are described in standard ISO-5821:2009 [15].

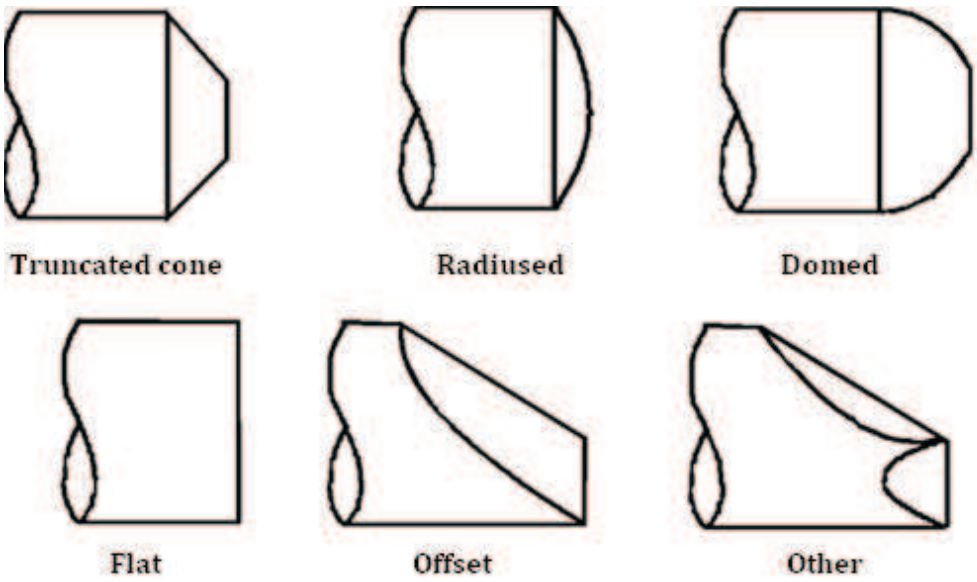

Figure 7 Electrode geometry types

2.3.5 Electrode material

The most important functions of the electrodes is to conduct electric current and to squeeze the sheets together. Therefore, electric conductivity, compressive strength and hardness are important factors in finding an appropriate electrode material. The material that fits the demands best is copper and copper-based alloys, as described in the standard ISO 5182:2008 [16].

The most common electrode material is a cupper-chromium-zirconium alloy, while higher resistance alloys of nickel, beryllium and/or cobalt may be used for higher strength steels and stainless steels.

2.3.6 Electrode degradation

Due to wear during repeated spot welds the electrodes suffers from degradation. Five degradation mechanics have been identified: softening, recrystallization, alloy formation, tip diameter growth and pitting. [17]

Softening is caused to the copper due to the repeated increased temperatures of the electrode during resistance spot welding. In turn, the softer metal will increase deformations and increase the tip diameter after sufficient welds. Recrystallization refers to the metallurgical process resulting of maintained higher temperatures of the electrode during the welding. Also, the contact with zinc during welding of coated steels will result in some alloying at the electrode tip to form brass. Pitting refers to the unevenness of the electrode tip after the above-mentioned

degradation mechanisms. The uneven tip will worsen weld conditions and increase risk of expulsion at the sheet-electrode interface. A heavily degraded electrode tip is shown in Figure 8.

In order to extending the electrode life a number of different measures can be applied. Most importantly, electrode dressing is used. It involves inserting the electrodes to a revolving metal cutter to remove typically about 0.1 mm to recover new cupper material. It is also possible to improve electrode degradation by optimizing weld parameters by keeping electrode forces low.

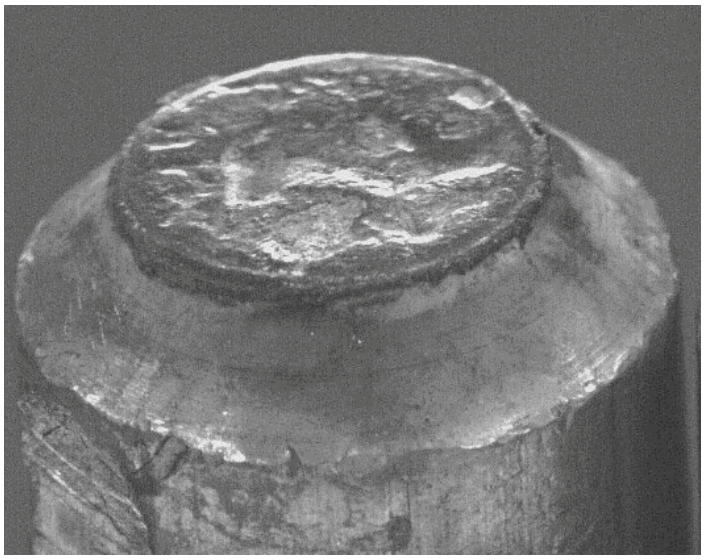

Figure 8 Example of a severely pitted electrode. [17]

If tip dressing is avoided, a concave tip will appear. In such extreme cases, only the perimeter of the tip is in contact with the sheet. As a consequence no heat is generated in the center of the electrode and the resulting weld will also have a ring shape - sometimes called a *donut weld*.

2.3.7 Other parameters

In production the parameters have been altered in certain ways to produce wished weld outcomes. These new techniques are variations of the elementary parameters described above but form a new frame work to produce certain desirable results in welding. They may improve the welding of certain material configurations or optimize the welding process.

Pre-pulsing is technique were a short duration, high current is passed through the materials before the actual welding current. Such a pre-pulse enables galvanizing

layers to be removed to enable better welding results during the actual weld time by improving sheet-electrode contact. It is also reported [18] to enable successful welding of more challenging sheet combinations, such as uneven thicknesses of multi-sheet stack-ups.

To improve nugget formation a continuously increase and decrease of current application has been proposed, also known as **up-slope current**.

2.4 Resistance spot welding equipment

Resistance spot welding is performed by weld guns which, holding the moving electrodes and connect them to the power source, which applies current. In the following Section, the different principles of weld guns are explained.

2.4.1 Gun types

Gun types can be defined according to a number of design principles. First of all, guns may be manual or automatic. Manual guns are operated by personnel and their performance is partly dependent on the welder. Automatic guns are installed on robots which are more precise in their welding but are more dependent on the geometry of the welded parts.

Another design aspect is the kinetics of the electrodes. Two main principles are used: pneumatic and electric guns. Electric guns are generally more powerful, more exact and more efficient but may be of a higher cost compared to pneumatically moving electrodes.

Also, the mechanics of the weld gun arms can differ. Two common alternatives are dominating, linearly moving electrodes, see Figure 9, and so called X-guns where the two arms are rotating along a common axis. An X-gun transfers the momentum at the axis to an electrode force at the electrode tips. Linear guns need less space and provide a pure axial force to the metal sheets but may also be more expensive compared to X-guns.

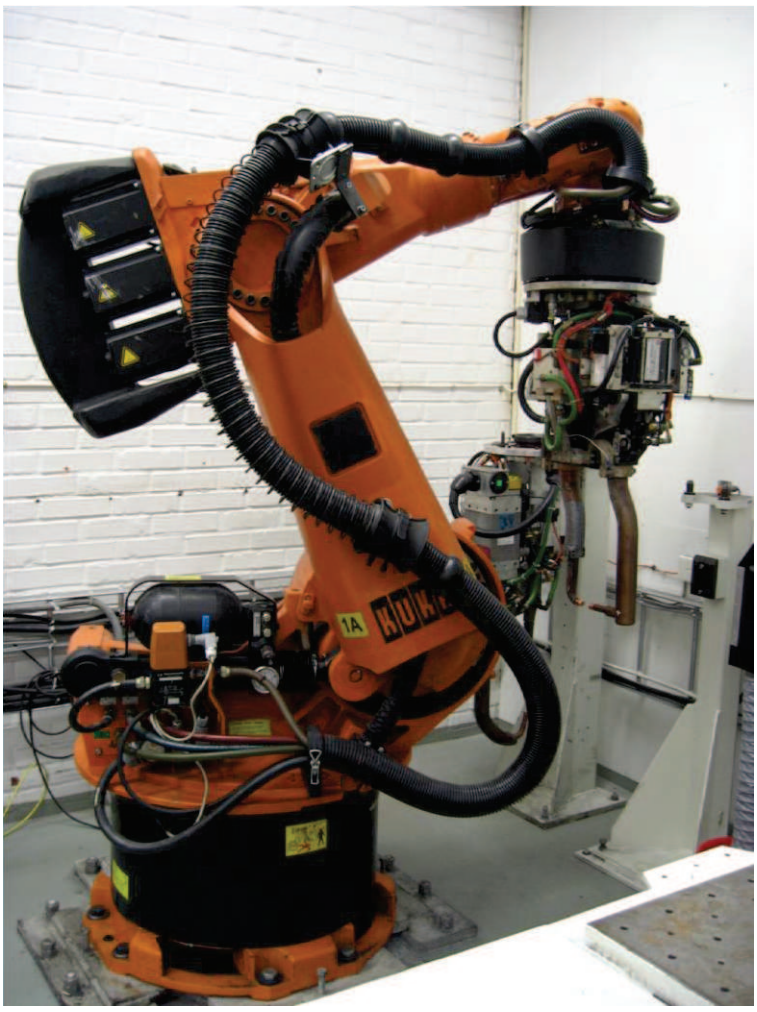

Figure 9 RSW linear gun attached to a robot.

2.4.2 Power sources

Traditionally, alternating current (AC) power sources were used for resistance spot welding. However, recently, direct current (DC) power sources have become more common. More specifically mid frequency direct current (MFDC) power sources are gaining popularity.

The reasons behind the development towards MFDC power sources are both increasing weld size and energy efficiency. Two identical set-ups with equal root-mean-square currents using AC and DC produce larger welds in DC mode, especially at lower currents. It is suggested that DC power sources create a larger contact resistance and thus more heat. Another reason is the electrical inductance caused

by the alternating current. In a case study comparing AC and MFDC power sources, it is suggested that the energy efficiency of MFDC is approximately 42% higher than AC power sources. In other words, 42% less energy is lost in the equipment. [19]

3 Physically based process planning of resistance spot welding

Process planning of resistance spot welding focuses on assuring of weld properties of process parameters before industrial production is started. In order to assure quality of established production and to examine new solutions, completed resistance spot welds are regularly tested and evaluated. Due to the uncertainties and largely automated and unmonitored production of spot welds, there is a great need for testing and verification of weld quality in the industry prior to large scale manufacturing.

Traditionally process planning has been performed through physical testing of weld properties. Physical testing of resistance spot weld tests can be divided into two categories: experimental tests under controlled environments and tests from industrial production. The experimental tests are often performed to examine a material configuration's weldability whereas production tests are made to assure weld quality of a configuration already in production.

In the following chapter, only weld geometries have been treated, i.e. tests of strength capacities or hardness tests have not been directly treated.

3.1 Evaluation criteria of resistance spot welding

To determine weld quality a number of parameters can be used as indicators. The following geometrical features are most commonly examined. [6]

- Weld nugget size
- Nugget penetration
- Electrode indentation
- Cracks (surface and internal)
- Porosity / voids
- Sheet separation / distortions
- Surface appearance
- Location accuracy

Many of the parameters are illustrated in the cross-section of Figure 10.

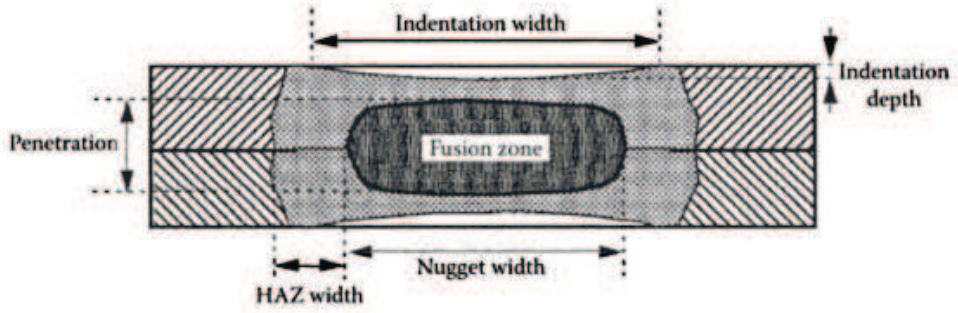

Figure 10 A typical cross-section of a spot weld and evaluation parameters. [6]

Of the parameters listed above, nugget size is the most indicative of weld strength and thus most frequently measured [6]. However, it is not sufficient to describe weld quality by itself and for a complete understanding of the properties of a weld several parameters needs to be measured. For example, penetration depth indicates the volume of material which melted during the weld process. Insufficient penetration indicates too low heat input while excessive penetration results in softening of the material and large indentation. Another, indication of weld penetration is the magnitude of the process margin. While, a larger penetration does not automatically result in higher strength, it shows that certain variations of weld output may be allowed with maintained results.

Literature mentions that corporations' standards and their requirements vary significantly due to their "drastic differences in design, understanding and perception of weld quality" [6]. As an illustration, requirements for nugget diameter from several organizations are compared in Figure 11. Requirements are doubled for certain configurations between manufacturers. Most requirements, however, demand a nugget diameter between $4\ \overline{d_{min}}$ and $5\ \overline{d_{min}}$., where d_{min} is the minimum thickness in the sheet stack-up. In industry, it is more effective to create a small amount of requirements, for example in table form, which hinders the use of such a general formula.

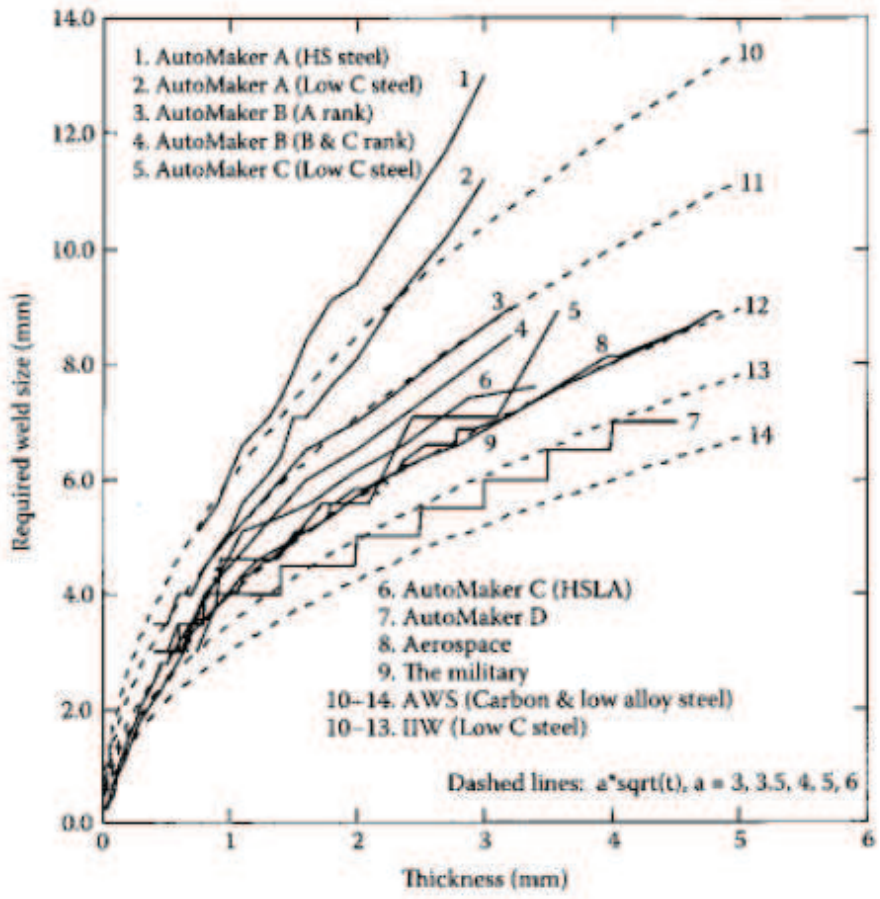

Figure 11 Weld size requirements from different organizations [6]

A similar comparison for penetration depth shows that requirement varies from less than 25% penetration of sheet thickness up to a minimum of 80% for certain military applications of aluminum welding.

3.2 Physical testing procedure

In order to find the relevant testing parameters for evaluation, an accurate, relevant and well-defined standard testing procedure should be carried out. Testing procedures can be divided into two main categories: destructive and non-destructive testing. The main destructive testing types are coach-peel tests and metallographic tests, as described below. Regarding non-destructive testing, the main types are by ultrasonic or x-ray but neither has reached the same level of accuracy or reliability as the destructive test methods [7].

Labs may conduct both experimental and production tests. Both are visually examined through metallographic testing to gain weld outcome. Hardness and mechanical strength tests can also be done to gather full understanding. Production tests are often, as mentioned earlier, samples from production and the welding process is not performed and controlled in a lab environment.

The experimental tests, on the other hand, are carried out on small coupons of standardized geometry. For each material configuration the weld current is step-wise increased for each coupon with two welds on each coupon. The double welds are performed in order to account for interfering shunt currents - the second weld is examined.

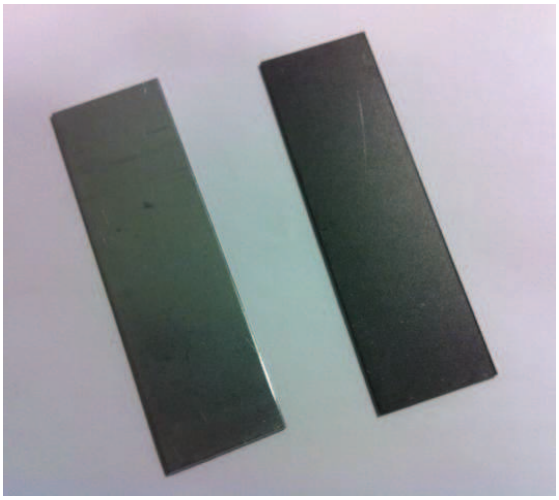

Figure 12 Test coupons for physical weld test.

The current is increased by 0.3 kA until repeated expulsion occurs to create a weld lobe. The current steps are repeated three times unless expulsion takes place. In expulsion occurs another coupon with the same configuration is done. A maximum of five coupons are performed for a specific weld configuration.

3.2.1 Coach peel testing

The most common method of physical testing is through coach peel tests were the specimens are manually peeled to reveal the weld zone or nugget [20]. The weld nuggets are measured using a digital caliper and both the minimum and maximum diameter is measured to account for non-circular weld zones.

The measurement is important and is needed to perform the evaluation of the weld properties in the size of the solidified zone.

Figure 13 Test coupon after coach peel test

3.2.2 Metallographic testing

The welded coupons are then cut through the center of the second weld. The rough surface of the cross-section is polished and chemically etched to reveal the material's micro structure.

The weld cross-section is then optically examined by microscopy and the relevant parameters are obtained and recorded by computer.

The main disadvantages and uncertainties involved in the described testing method are those involved with in using a 2-d test surface to describe the properties of a 3-d weld volume. A center cross-section may not show all properties of the entire weld, such as porosity, voids or other imperfections.

3.2.3 Documentation of physical testing

From the gathered data, three to five welds are performed for a certain weld current. Thus, a relation between weld outcome and welding current for the specific material configuration can be established. The resulting range of currents which gives satisfactory welds is known as a welding lobe.

The range of a welding lobe is defined by the minimum requirements and by an expulsion current. A 1-d weld lobe, where only the current is varied is shown in Figure 14.

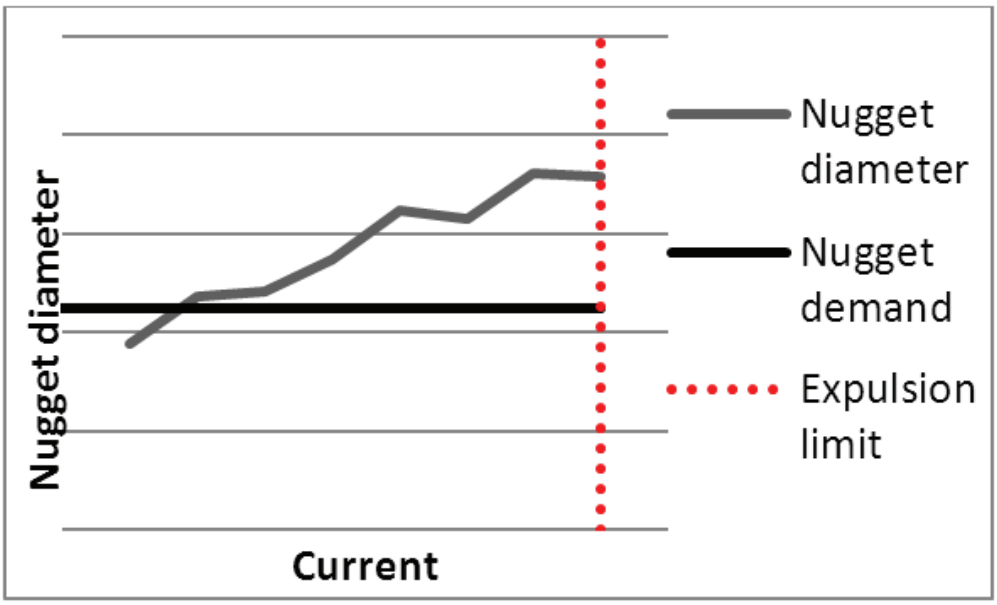

Figure 14 A typical 1-d weld lobe showing the accepted weld current range.

A 1-d weld lobe is a concise illustration of the weldability of a material configuration, making it ideal for many industry purposes. 2-d weld lobes in which both current and weld time or electrode force have been varied can also be used.

4 Model based process planning of resistance spot welding

In order to replace physical based process planning of RSW, several models can be used. In the present thesis regression models and finite element models have been studied. The two modeling approaches are treated in the present chapter.

4.1 Regression models of RSW

Regression models are a numerical model which uses statistical relations between a known set of input parameters (X) and output result (Y) to form a general model between the two general sets (x, y) with a set of constant coefficients (c). A regression model may be in the form shown in equation (2).

$$y = c_1 x_1 + c_2 x_2 + \ldots + c_n x_n \quad (2)$$

Regression models of the RSW process have to some degree been subject to research [21], [22], [23]. However, these models only treat only one material each and are thus not ready for a larger scale industrial implementation.

The regression model is generated through a least-square fitting, by the known set of input data and results, (X, Y) as shown in equation (3) [24].

$$c = (X^T X)^{-1} X^T Y \quad (3)$$

In in equation (3), the matrix X includes the known factors and the matrix Y includes the known results.

In RSW process planning, the most important measurement is weld nugget size and its sensitivity to process parameters. Thus, the regression model should describe the effects of changes in process parameters to weld nugget size. The benefits of a regression model is the mathematically simplicity of the numerical model, while having high predictive capability if generated correctly.

The factors known to affect the weld nugget size are many and are often dependent of each other. The factors included in the regression model should satisfy several qualities; they should be physically and statistically significant while being easily accessible for process planning.

The effect of different factors on the weld size and thus their relevance in the regression model can be evaluated by ANOVA (ANalysis Of VAriance) [24]. ANOVA

is a set of statistical tests used for evaluation of data. For the present work, two ANOVA tests have been used; the F-test and the t-test. The F-test is designed to evaluate the significance of all factors of the model in one test. The t-test is designed to evaluate the individual factors of a test. In order to gain a statistically significant both tests should give successful test results.

4.2 Finite element modeling for RSW simulations

Due to the complex multi-physical phenomena in the RSW process the FE simulations must be carefully formulated. More specifically, the coupled electrical-thermal-mechanical coupling is of particular concern. In the following Chapter, the general modeling approaches and coupling, the governing equations of the model and the boundary conditions of the mesh are presented.

The first research work in RSW modeling [25] focused on one-dimensional models of the temperature distribution of the RSW process. Later the first axi-symmetrical model was developed [26]. Later axi-symmetrical models also measured the contact diameter between the sheets [27]. Research continued with a one-dimensional model which took the temperature dependence of resistance into account [28]. Other axi-symmetrical models took the contact pressure dependence of contact resistance [29] or the steel hardness dependence of contact resistance [30] into account. A one-dimensional model was developed which measured weld size through temperature dependent contact resistance and material properties [31]. These earlier models were based on the Finite Difference Method, which limited their accuracy.

Development continued with models based on the Finite Element Method with constant material parameters and a fully elastic mechanical model [32] and an elasto-plastic model [33], [34], [35]. Later, coupling of the thermal, electrical and mechanical fields was introduced in simulations [36], [37]. Also, research was published which focused on 3d-models of RSW [38]. Models were developed with more detailed analysis of contact resistance conditions [39], [40] [41]. Work was focused on modeling of steel sheets, but research treating aluminum sheets was also introduced [42]. Due to the large and rapid temperature variations during the RSW process, metallurgical modeling was later introduced [43],

Due to some specific non-linear features of RSW simulations, such as complex contact phenomena and multi-physical coupling, RSW simulations are to some point limited to a few designated FE software. The software Sysweld [44] [45], Sorpas [46], JWRIAN [47] and SpotSim [48] are developed specifically to simulate

RSW simulations. In the present thesis, Sysweld and Sorpas have been studied and used and the modeling is based on these software.

4.2.1 General modeling approach

In the following Chapter the most general modeling approaches are presented. The models are based on the FE code SYSWELD but are general and can be used in other codes.

4.2.2 Geometry and mesh

In the spot weld simulations, most simulations are done using an axi-symmetrical model. The axi-symmetrical model will decrease the number of elements compared to a full 3-d model. However, asymmetrical irregularities may not be modeled. The elements have two displacement degrees of freedom (radial and vertical direction), a temperature degree of freedom and a voltage degree of freedom.

4.2.3 Electro-thermal-mechanical coupling

In practice the coupled models are executed in small time-steps where, in each time step, the electro-thermal computations are made and used as input for the thermo-mechanical computations. A schematic illustration of the coupling can be seen in Figure 15.

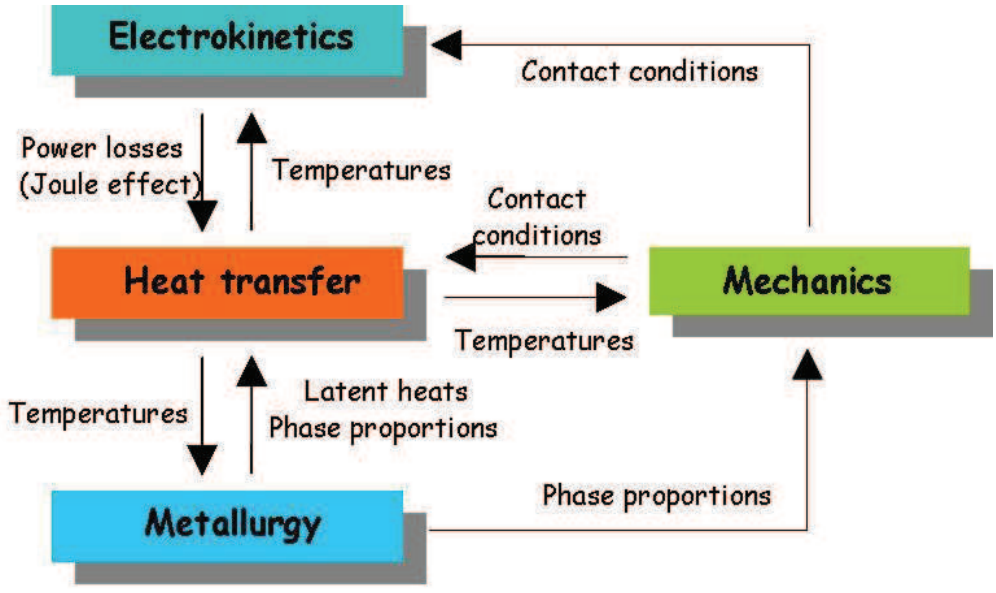

Figure 15 Coupling of RSW FE simulations. [45]

4.2.4 Modeling and boundary conditions

In the simulations, a number of principal constitutive relations control the outcome of the simulations. These consecutive relations are often coupled but may still be defined individually. In the below section, the constitutive relations which control the simulations are treated. They have been grouped into thermal, electrical and mechanical modeling principles. In addition, each governing equation is controlled by a set of boundary conditions, presented in chapter 4.2.8.

4.2.5 Electrical governing equations

As the main source of heat, due to the Joule heating, the electrical governing equations are presented first. To model the RSW process the steady-state electro-kinetic problem can be used as an initial approach. The steady flow of current between the electrodes can be stated by Ohm's law in vector form, equation (4).

$$J = \kappa \nabla V \tag{4}$$

The current of a specific cross section of area s is calculated as in equation (5).

$$I = \int_s J ds \tag{5}$$

In tandem with the principle of conservation of current flux, see equation (6), the above equations form the base of the electrical model.

$$\nabla J = 0 \tag{6}$$

4.2.6 Coupled electro-thermal modeling equations

Due to the non-steady state of the RSW process the electrical model must be coupled to the thermal model to achieve accurate results. The formulation of the internal heat distribution of a body is shown in equation (7).

$$\rho \frac{\partial H}{\partial t} - \nabla \left(k \nabla T \right) - \nabla V \left(R \nabla V \right) - Q = 0 \tag{7}$$

The first term includes the enthalpy and the density of the system. The second term includes the conductive heat and the third term is the Joule heating term. The fourth term includes the internal heat generation.

It is of importance to note that in the RSW process thermo-electrical phenomena such as the Thomson or Peltier effects take place. However, the mentioned effects

are not included in the model due to their small effect. Mathematically expressed, the term Q is neglible.

Another aspect worth noting is the distinction between enthalpy and specific heat - both properties describe the thermal state of the body. However, to fully take phase transformation effects into account accurately, the enthalpy model is more convenient.

4.2.7 Mechanical modeling equations

Given the computations of the electro-thermal modeling equations, the results can be used for the mechanical model. To establish the mechanical model the compatibility condition of the FE formulation is stated as in equations (8) and (9), respectively, representing normal and shear strains.

$$\varepsilon_r = \frac{\partial u_r}{\partial r}\,, \varepsilon_\theta = \frac{\partial u_\theta}{\partial \theta}\,, \varepsilon_z = \frac{\partial u_z}{\partial z} \tag{8}$$

$$\gamma_{rz} = \frac{\partial u_r}{\partial z} + \frac{\partial u_z}{\partial r} \tag{9}$$

The governing equation of the mechanical model can be expressed as in equation (10), representing a conventional elasto-plastic model.

$$\Delta\sigma = \ D\ \Delta\varepsilon + [C]\Delta T \tag{10}$$

The matrices [D] and [C] describe the elastic and thermoelasto-plastic states, respectively.

4.2.8 Boundary conditions

In parallel with the governing equations, the model is based on a set of boundary conditions for the thermal, electrical and mechanical models. Each is treated separately below.

4.2.9 Electrical boundary conditions

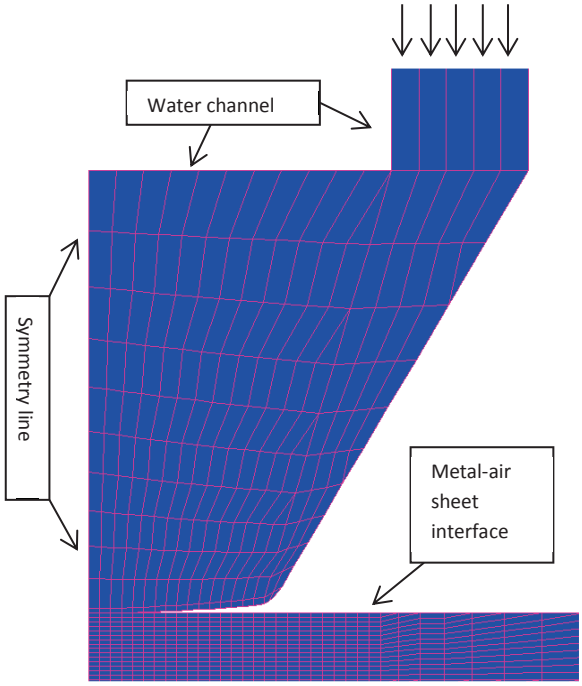

Figure 16 Boundary conditions associated with RSW FE simulations in SYSWELD

The electrical boundary condition is a formulation of the applied welding current and the physical boundaries of the sheet, as shown in the following equations.

At the water channel	$J = 0$	(11)
At the symmetry line	$J = 0$	(12)
Top of upper electrode	$V = V_e$	(13)
Bottom of lower electrode	$V = 0$	(14)
At the metal sheet surface facing air	$J = 0$	(15)

4.2.10 Thermal boundary conditions

The thermal boundary conditions are defined according to the following Equations.

Heat loss at electrode-water interface.

$$-k\frac{\partial \mathrm{T}}{\partial n} = K(T_w - T) \qquad (16)$$

n is the normal direction of the boundary. The function *K(T)* is a combined function of the convection heat transfer coefficient and the radiation heat transfer coefficient.

Heat loss at metal sheet surface to air.

$$-k\frac{\partial T}{\partial n} = K(T_\infty - T) \qquad (17)$$

T is the temperature of the surrounding medium, i.e. the air temperature. In the Sysweld model, *K(T)* includes both convective and radiation heat transfer closer to the electrodes but only convective heat transfer further away from the electrodes.

At symmetry lines.

$$-k\frac{\partial \mathrm{T}}{\partial n} = O \qquad (18)$$

4.2.11 **Mechanical boundary conditions**

The mechanical boundary conditions are defined according to the following equations.

The pressure on the top of the upper electrode.

$$\sigma = -q \qquad (19)$$

The displacements at the bottom of the lower electrode.

$$u_z = 0 \qquad (20)$$

The displacements at the symmetry line.

$$u_r = 0 \qquad (21)$$

The stresses at the metal surfaces.

$$\sigma = 0 \qquad (22)$$

4.2.12 **Boundary conditions after welding**

As the hold time is finished and the electrodes are removed from the sheets a new set of boundary conditions are applied to the model. Firstly, the radiation component of the sheet surface heat transfer is neglected over the entire sheet, not only far from the electrodes as during welding. Secondly, the electrical contact condition is removed. Thirdly, both electrodes are set to a vertical displacement of 3 mm away from the sheets.

5 Results and discussions

To answer the research questions in chapter 1.3 a number of studies have been performed. The results from these studies and answers to the research questions are summarized in the following chapter. A more detailed description of the studies is included in the appended papers.

5.1 Variations of resistance spot welding

In RSW, the diameter of the weld nugget, the solidified joining interlayer between sheets, is the main measure of weld quality and functionality as described in chapter 3.1. However, with nominally constant weld process parameters, sheet materials, geometry and other controllable variables the weld nugget diameters have been seen to vary between welds. The magnitude, distribution and causes of such variations are partly unknown and a clear analysis is yet to be done.

An analysis was performed to quantify and analyze the variations of weld quality in RSW applications. As a collection of results for analysis, controlled laboratory welding and production welding were carried out. Several apparently identical welds were used for analysis.

The laboratory trials were welded with two coupons of rephosphorized steel, a common material in automotive production. For the production welds, three joints, which all included two sheets of rephosphorized steel sheets, were selected.

All welds were destructively tested using coach peel tests and weld nugget sizes were measured and recorded. The results of typical standard deviations of the series from laboratory and production environments are shown in Figure 17.

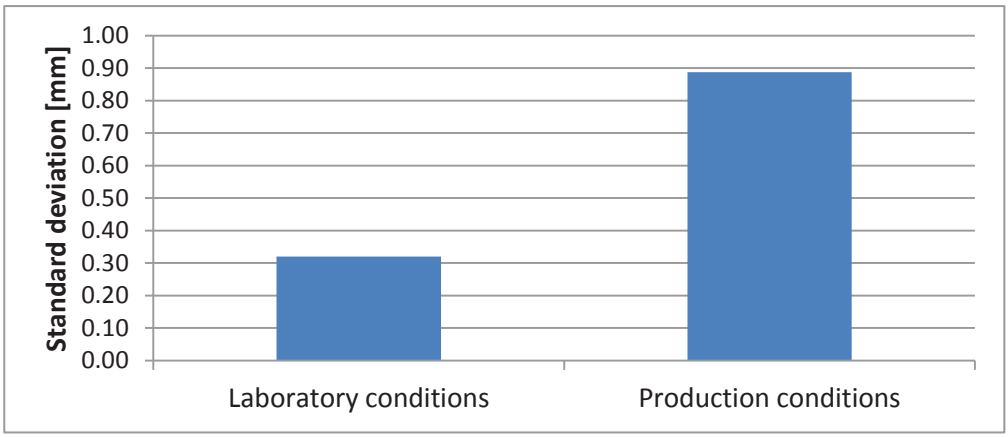

Figure 17 Standard deviations of typical RSW results.

To predict weld sizes more accurately, it is of interest to examine the distributions of the weld sizes. Also, fitting of a conventional probability distribution has been performed and evaluated by X^2-tests. The results of the X^2-tests show that both Weibull and normal distributions show good fit to the weld size results with both laboratory and production welds.

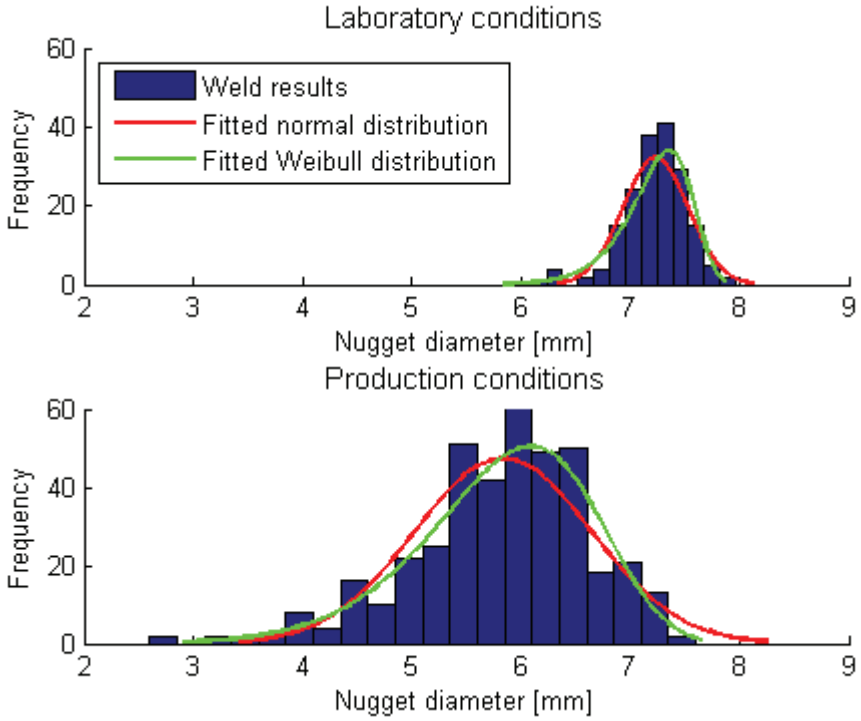

Figure 18 Distributions of typical RSW results.

The results of the present studies can be used to draw a number of conclusions about variations of weld nugget. Typical standard deviations of resistance spot weld nugget sizes in laboratory environments are approximately 0.30 mm in magnitude. Typical standard deviations of resistance spot weld nugget sizes in production are approximately 0.90 mm in magnitude. Moreover, results show that both fitted normal and Weibull distributions show promising results in describing weld size distributions.

5.2 Regression models of resistance spot welding

In RSW process planning it is of interest to determine the effect of weld parameters on weld sizes. By understanding such effects, parameters and welding equipment can be optimized for maximized weld sizes and maintained process robustness.

While, conventional physical evaluation and optimization is costly and time consuming virtual tools, which are faster and less costly, can be used. One such method is regression analysis which has been successfully used for other manufacturing processes. By using regression analysis, results from previous testing can be used to predict general welding results.

In the present thesis, general regression models for RSW weld prediction have

been generated. The input for the models is results from physical testing, which has been carried out for an extensive range of materials and equipment in modern RSW applications. In total, over 200 spot weld results have been used for analysis.

The models predict weld nugget diameter, which, as described in chapter 3.1 is the most common measure of weld quality. In the analysis weld parameters such as weld current and electrode force, equipment parameters such as electrode tip area and material parameters such as material thickness. The distributions of weld parameters are shown in Figure 19. Both linear and quadratic terms have been used for the analysis.

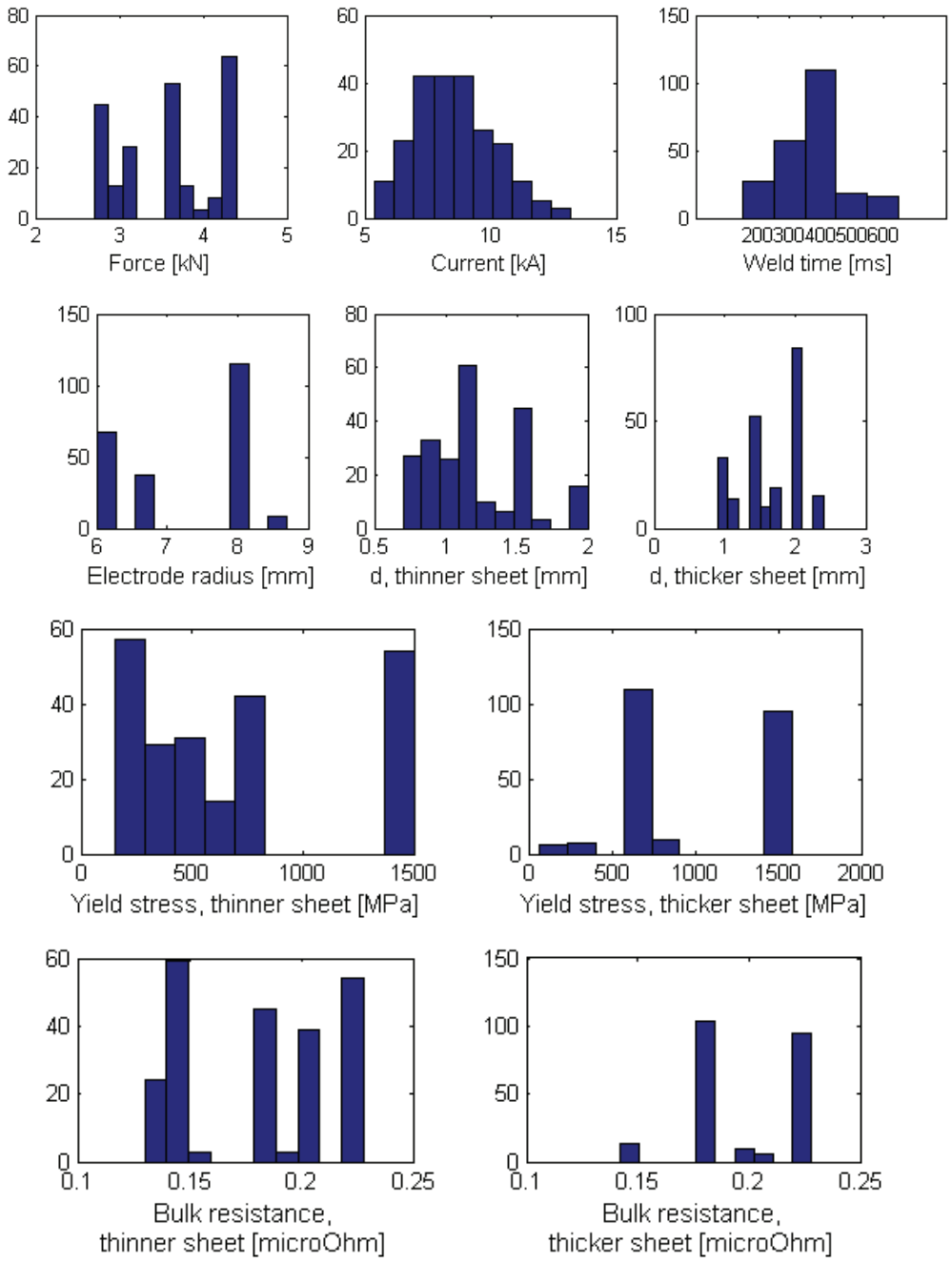

Figure 19 Distributions of input parameters for regression models.

Three different regression models were generated using iterative step-wise regression methods. The methodology of the iterative step-wise regression is shown in Figure 20 and is based on Analysis of Variance (ANOVA) and adjusted R^2-value [24]. The first model included pre-selected factors which were forced to be

included in the model. The second and third model included linear and quadratic terms, respectively, without any pre-selected factors.

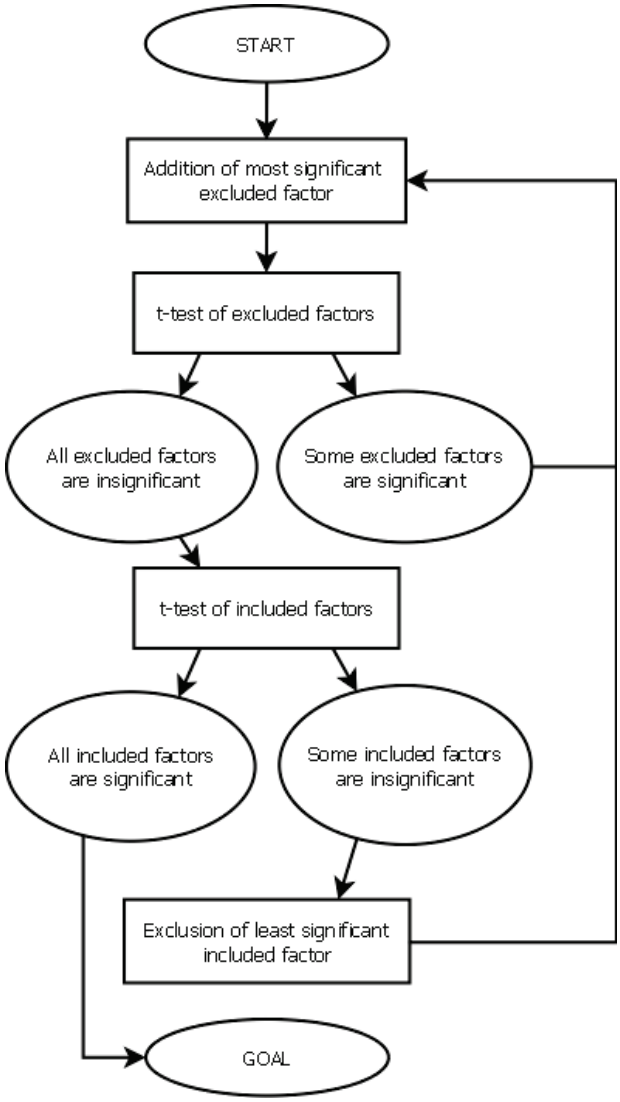

Figure 20 Step-wise regression methodology

All models gave successful results in terms of ANOVA tests, which indicate the models are statistically significant. However, the models gave somewhat different results in terms of factors included in the model, despite the successful ANOVA tests.

The various selected factors of the models indicate the complex behaviour of weld growth during RSW. It also indicates the dependency of many physical phenomena in weld nugget growth.

The forced, or pre-selected model, resulted in the highest R^2-value, thus indicating the highest predictive capability. Secondly, the linear model showed the lowest predictive capability indicating that linear terms do not capture the weld results to as high degree. The quadratic model showed intermediate predictive capability. However, the quadratic model has the lowest number of factors compared to the other models, which may be advantageous in engineering use. The standard deviation of the error, which also is a measure of the predictive capability is similarly ordered; the forced model has the lowest standard deviation (0.5 mm) followed by the quadratic (0.6 mm) and the linear model (0.7 mm). The regression model results compared to the physical results are shown in Figure 21, Figure 22 and Figure 23, respectively.

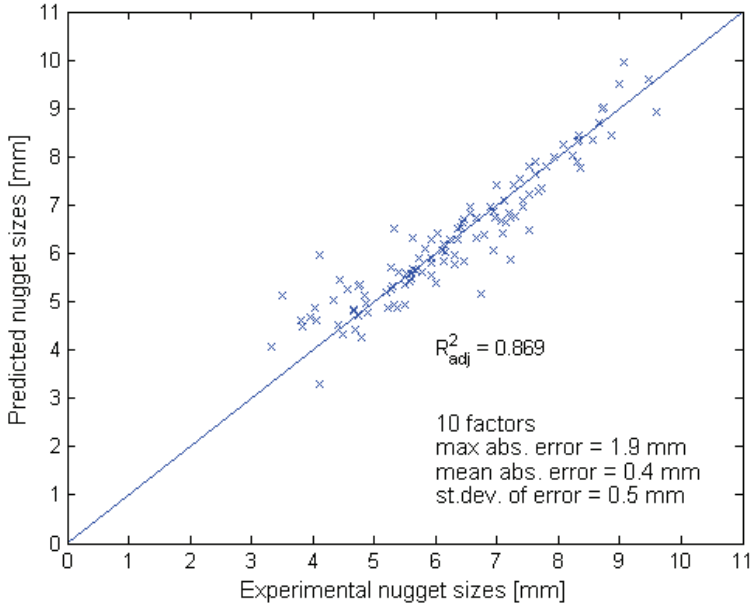

Figure 21 Regression accuracy of forced model.

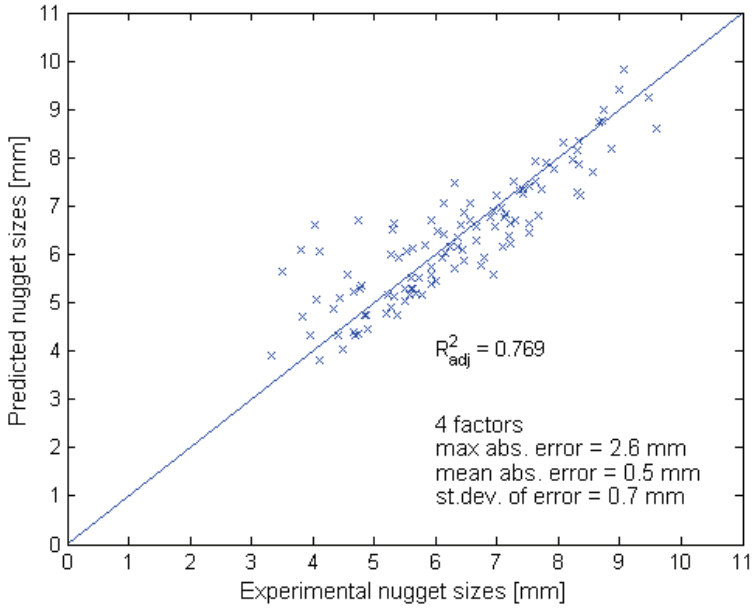

Figure 22 Regression accuracy of linear model.

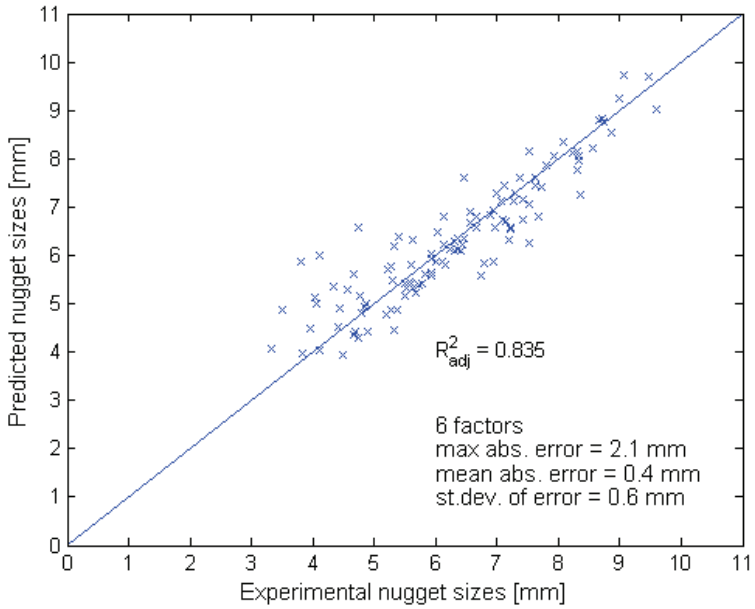

Figure 23 Regression accuracy of quadratic model.

5.3 Material models for simulations of resistance spot welding

In order to perform FE simulations of the spot welding process, multiple material data are needed for the governing model. To make the simulations sufficiently accurate, the material data must be defined as functions of both temperature and phases for each material. For the present studies of RSW, the models for the base material microstructure and the austenite microstructure are relevant. The transition between base material and austenite models were modeled from the Ac1 and Ac3 temperatures, which were gained from experiments.

In the following part, the material data for the selected materials are presented. The method of gathering the data and data evaluation is also presented through standard deviations compared to experimental data where relevant. In some cases generalization have been made, which are also presented.

5.3.1 Sheet and material scope

A number of materials commonly used in automotive industry are evaluated for material data. Table 1 shows the materials, sheet thickness and coatings of the selected materials. The material list covers a wide range of materials from ultra-

high strength steels, such as boron steel or martensitic steels, to lower strength steels, such as Dogal 260, which is a rephosphorized steel.

Table 1 Sheet specifications of simulation materials

Sheet material	Coating layer	Thickness
Boron steel	AlSi	1.50 mm
Rephosphorized steel	Uncoated	1.50 mm
DP600	Z75	1.25 mm
DP800	Z75	1.50 mm
DP1000	Z75	1.50 mm
Martensitic steel	Z75	1.30 mm

5.3.2 Thermal data

The thermal properties of the FE model are governed by several properties; the thermal conductivity, the specific heat and the thermal expansion. Below, the different properties are treated separately.

5.3.2.1 Thermal conductivity

The thermal conductivity is calculated using the software IDS, which uses the alloying elements of the material to gain the properties for each temperature. The thermal conductivity of the alloying elements is weighted against the thermal conductivity of pure iron in the calculations. The weighing factor is not constant but dependent of temperature.

From the results from IDS linear or second order regression models were built for general expressions of thermal conductivity for all materials and temperatures. A common model for base material and austenite was used.

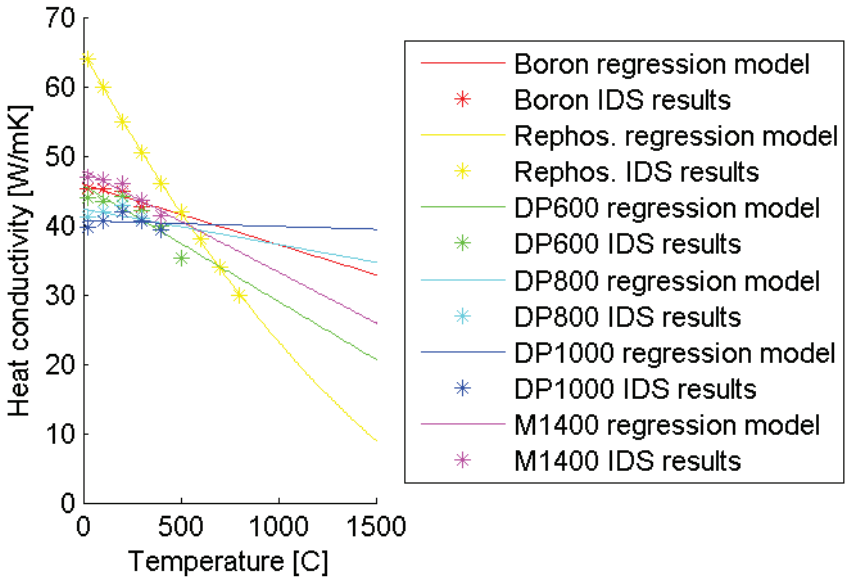

Figure 24 Thermal conductivity model.

5.3.2.2 Specific heat capacity

Specific heat capacity was simulated using the software ThermoCalc for all materials and micro-structures based on thermodynamic equilibrium. ThermoCalc calculated the specific heat from the alloying contents in the materials. The Thermo-Calc calculations are based on the relation between Gibbs free energy, enthalpy and entropy of the system.

For the simulations, linear interpolation was used between the data points obtained from ThermoCalc. A common model for base material and austenite was used.

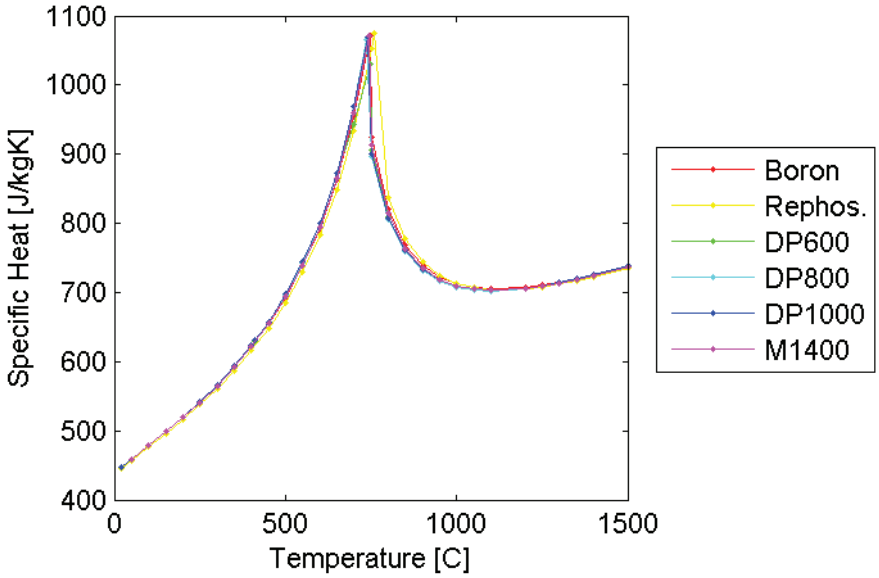

Figure 25 Specific heat model.

5.3.2.3 Thermal expansion

The data for thermal expansion is generated from dilatometer experiments where the temperature of a test specimen was controlled and the volume changes were measured. The temperature was elevated and reduced in order to gain all three relevant micro-structures of the material

Since the deviations between materials were small a general model was used for simulation for each microstructure. Also, the thermal expansion coefficient is considered to be independent of temperature. The coefficient of thermal expansion used in simulation was 1.38e-5 for the base material and 1.96e-5 for austenite.

5.3.3 Mechanical data

The mechanical model in the simulations is controlled by four parameters; Young's modulus, Poisson's ratio for the elastic deformations, a flow stress deformation curve for the plastic behavior and yield stress to govern the transition between elastic and plastic behavior.

In order to obtain the material data, several specimens of each material were tensile tested at different temperatures and micro-structures. Tensile testing was performed to gather the engineering stress and strain. The raw data is test

specimen specific and not material general and must be converted into true stress and strain for model generation.

5.3.3.1 Young's modulus

The Young's moduli data were obtained using least-squares linear regression of values between two stress values. The two stress values are obtained semi-empirically by selection of an upper limit of fully elastic behavior. The data between 25% and 75% of the selected stress value are used for linear regression to obtain the Young's modulus.

For the simulations, a common Young's modulus model has been used for all materials and all micro-structures. A linear approximation, as seen in Figure 26 has been used. The linear approximation is valid up to a threshold value, which is 1% of the value at room temperature. At temperatures above the threshold value, the Young's modulus has been modeled as constant. The standard deviation between the model and the experimental results was 26.7 GPa.

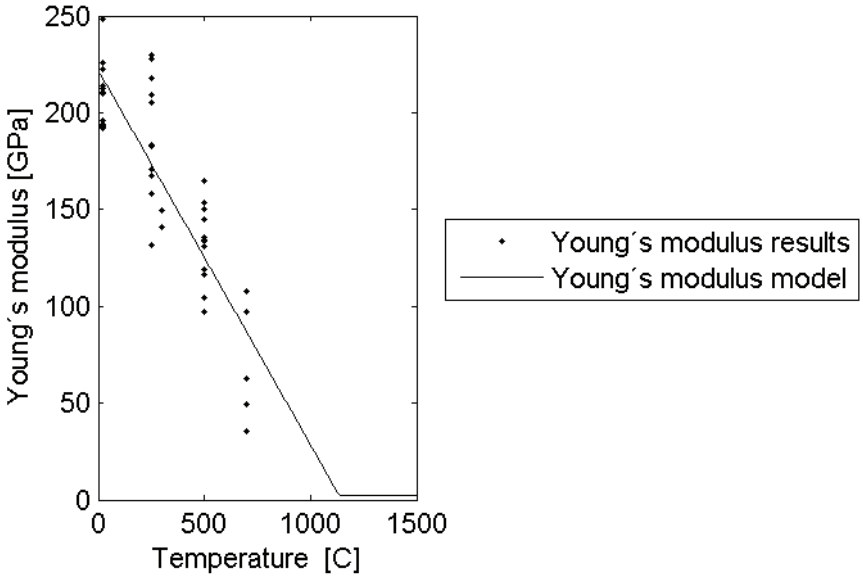

Figure 26 Young's modulus model.

5.3.3.2 Poisson's ratio

In the present study, the Poisson's ratio, which models the contraction of the material, is considered constant for all materials, temperatures and phases at 0.3. No physical testing has been done to evaluate Poisson's ratio.

5.3.3.3 Yield stress

The yield stress determines the transition between elastic and plastic behavior in the mechanical model. The processing of tensile test data to obtain the yield stress used the Young's modulus approximation, described in Chapter 5.3.3.1. The Young's modulus will create a linear stress-strain curve, which in the elastic region is near identical to the test stress-strain curve. However, as the plastic deformations take place, the perfect linear curve and the test curve will start to deviate. A conventional method of defining a yield stress is by locating a specific divergence between the two curves, i.e. a specific plastic strain magnitude. In the present work, the yield stress is defined as the stress where the plastic strain is 0.2 %.

For yield stress, several approaches were evaluated to generate a general model for simulations; a linear interpolation model, a linear regression model similar to the Young's modulus model and Johnson-Cook models [49]. It was concluded that the linear regression model was the most accurate in modeling yield stress. The yield stress models are shown in Figure 27. The standard deviation between the model and the experimental results was between 60.8 MPa for the DP600 material and 137.0 MPa for the martensitic steel.

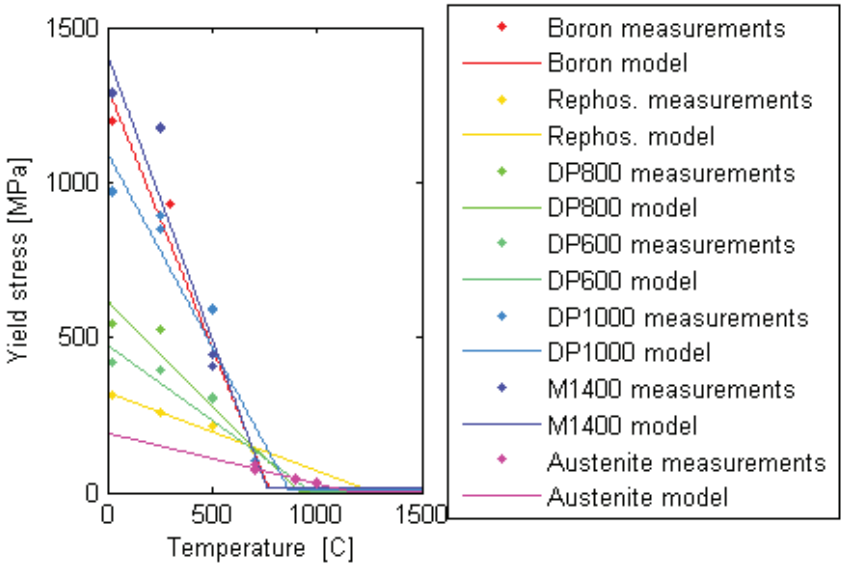

Figure 27 Yield stress model.

5.3.3.4 Flow stress

The flow stress describes the plastic behavior, i.e. the deformations above the yield stress limit. The true test stress-strain curves from the tensile tests have been used to establish a general material model for the plastic behavior for simulation. To establish the general model for all temperatures both Johnson-Cook models and a parameter optimization were evaluated.

The parameter optimized stress-strain relation showed very high correlation to the test data while the Johnson-Cook models were found to be insufficient. The optimization method used MATLAB Optimization Toolbox [50] to fit the parameters B and n in Equation (23) to the tensile test results..

$$\sigma = \sigma_Y + B\varepsilon_{pl}^{n} \tag{23}$$

After the optimization, the standard deviation between the model and the measured stress-strain curve was between 0.66 MPa and 79.15 MPa. The flow stress curves are seen in Figure 28. Additionally, no deformation hardening took place at temperatures above the melting temperature

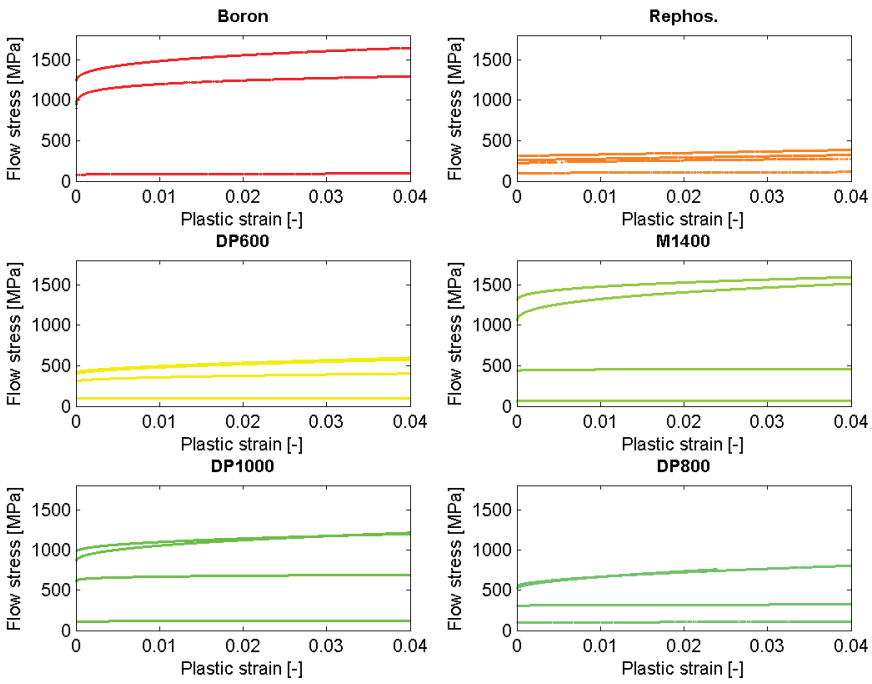

Figure 28 Flow stress models.

5.3.4 Other material data

In resistance heating, the electrical properties of the sheet materials are of high importance. For the electrical model, the electrical conductance is used as input data. The electrical conductance will control the Joule heating of sheets in the simulation. The electrical conductivity is controlled by a master curve, which is common for all materials and phases [45].

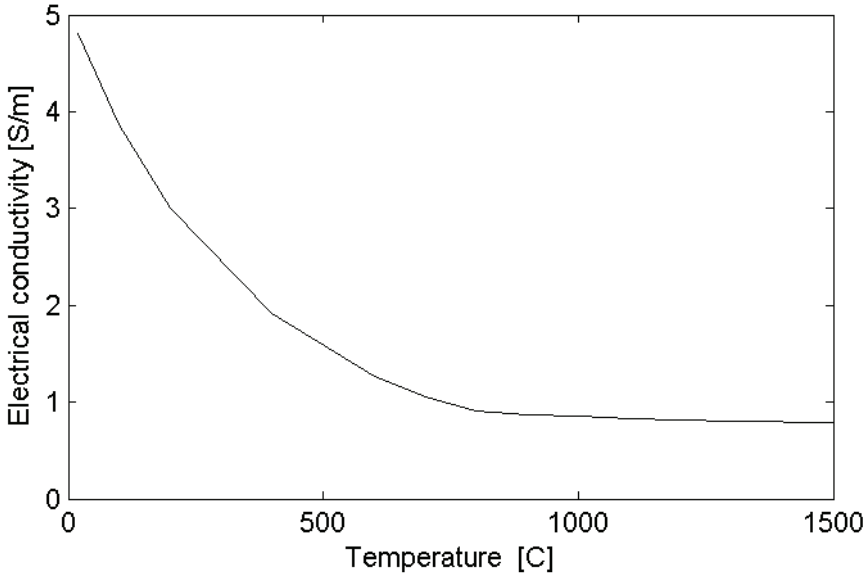

Figure 29 Electrical conductance model.

The density of the materials is defined by a common model used for all materials and micro-structural phases and uses linear interpolation between two given values; 7815 kg/m^3 at 20C and 7290 kg/m^3 at 1500C.

For the contact conditions, a element layer of specific thermal and electric contact conductances was included in the model. The conductances used a general model for all materials and were dependent of temperature. [45]

5.4 Physical verification of resistance spot welding FE simulations

The material data models shown in chapter 5.3 were used for FE simulations in order to verify simulation methods by physical testing. The same six materials as in the previous chapter were analyzed in 2-sheet stack-ups. Each material generated a 1d-lobe with varying current and constant electrode force and weld time.

The physical experiments generated weld nugget sizes for each current and material and the occurrence of expulsion. The welding was performed on smaller sheet coupons and two welds were welded on each coupon stack-up. The two welds would analyze the effect of shunting currents to the previous welds.

The FE simulations calculate the weld nugget size as the size of the molten zone at the interface at the end of the weld time. Also, the simulations gave an expulsion limit based on the weld zones contact with the air gap. The simulation does not take shunting into regard

A comparison between weld sizes from simulation and physical welding can be seen in Figure 30. The standard deviation of the residual between the weld size diameter of the FE model and the experiments is 0.68 for all welds. The first weld is more accurately modeled with a standard deviation of 0.54 mm compared to 0.80 for the second weld. As seen in chapter 5.1 standard deviation in experimental welding is approximately 0.3 mm.

By treating the expulsion occurrence as a discrete probability distribution the experiments give an expected value of the expulsion limit. The expected value can be used for comparison to simulations. The comparison is illustrated in Figure 31.

The comparison shows that the standard deviation of the residual of the expulsion limit is 1.27 kA. The values for the first and second weld location are 1.15 kA and 1.27 kA, respectively. I.e., the expulsion limit better capture the expulsion of the first weld location.

Expulsion limits has variations in physical testing just like weld sizes. The standard deviation of the expulsion limit in physical testing can be measured by the discrete probability distribution. The standard deviation of expulsion limit is 0.21 kA considering both weld locations and all materials.

The present results show the capability of RSW FE simulations. Compared to many other comparable studies, the present work has an extensive scope of physical experimental results. The extent of the comparison shows the benefit of FE simulations for industrial implementations.

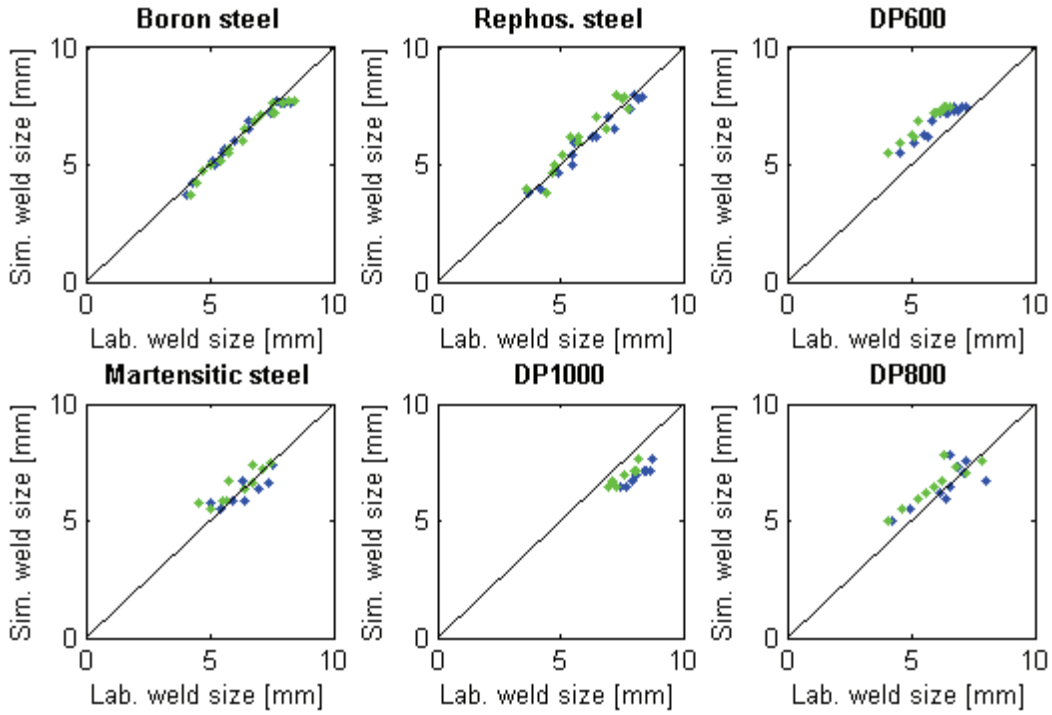

Figure 30 Results from simulations and physical testing of weld nugget size for all materials of welds from the first weld location (blue) and second weld location (green).

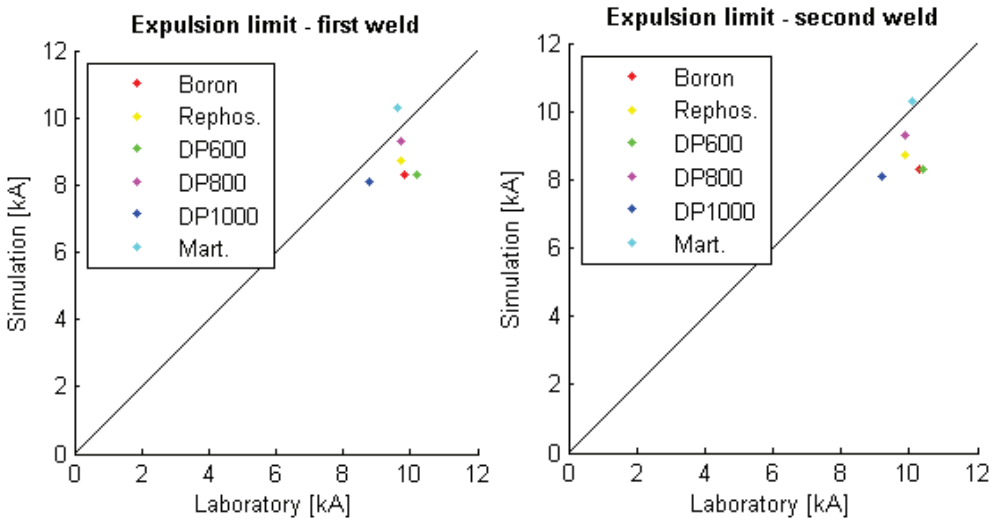

Figure 31 Results from simulations and physical testing of expulsion limit.

6 Conclusions and future research

The following chapter shows the main conclusions from the present thesis and presents directions for future research work.

6.1 Conclusions

The present thesis focuses on process planning of resistance spot welding. A number of studies have been carried out to answer research questions regarding variations of spot weld sizes and predictive capability of numerical methods of the RSW process. A number of conclusions can be drawn from the studies.

Firstly, variations of RSW weld sizes were statistically analyzed. The studies showed that under apparently identical conditions, weld sizes vary by a significant magnitude. The magnitude of variations was also seen to be different between controlled laboratory conditions and production conditions. The standard deviation of laboratory welds and production welds were approximately 0.3 mm and 0.9 mm, respectively.

Also, the studies of weld size variations showed the distribution of weld sizes. It was seen that both in laboratory and production conditions, both normal and Weibull distributions could describe the distribution of weld sizes.

Further studies analyzed numerical methods of the RSW process by both regression models and FE simulations. The numerical methods were evaluated by comparison to physical welds. Both models showed promising results by physical verification. The standard deviations of the regression models were in the order of 0.5 mm to 0.7 mm and for the regression models and in the order of 0.7 mm for the simulations

For the FE simulations, material models for several materials were generated. The models included thermal, mechanical and electrical data for elevated temperatures. The models were generated by means of material simulation, material testing and literature studies.

6.2 Future work

The present thesis includes knowledge regarding the process planning of RSW. The results from the thesis also identified future work for research.

The first part of the thesis included analysis of variations of RSW weld sizes. A key conclusion form the results was the difference in magnitude of variations between

laboratory and production conditions. While, variation in spot weld location, through shunting currents, were seen to be a source for the difference, other sources are possible. To further minimize variations, it is of interest to establish and quantify other disturbance sources, such as geometrical variations and variations in weld equipment condition

Regarding the numerical models, both regression and FE models, the results showed their predictive capability. While, the verification was performed on 2-sheet joints of similar materials, current industrial application often include joints of more than two sheets and often of dissimilar materials and thicknesses. In order to fully evaluate the capability of the methods, it is interest to verify with a larger scope of different joints.

Furthermore, it would be of interest to improve the modeling of the expulsion limit. In initial step would be to increase the resolution of the current parameter. In the present work, steps of 0.3 kA were used. However, the relatively large steps resulted in large standard deviations of results. By decreasing the steps a more detailed analysis could be performed.

7 References

[1] S. Oberthür and H. Ott, The Kyoto protocol, Berlin [u.a.]: Springer, 1999.

[2] P. Nieuwenhuis, A. Beresford and A. K.-Y. Choi, "Shipping or local production? CO2 impact of a strategic decision: An automotive industry case study," *International Journal of Production Economics,* vol. 140, no. 1, pp. 138-148, 2012.

[3] R. H. Borcherts, H. L. Stadler, W. M. Brehob and J. E. Auiler, "Improvements in Automotive Fuel Economy," *Energy,* vol. 3, pp. 439-449, 1978.

[4] A. Topolansky, "Alternative fuels: Challenges and opportunities for the global automotive industry," *The Columbia Journal of World Business,* vol. 28, no. 4, pp. 38-47, 1993.

[5] K. Edwards, "Strategic substitution of new materials for old: Applications in automotive product development," *Materials & Design,* vol. 25, no. 6, pp. 529-533, 2004.

[6] H. Zhang and J. Senkara, Resistance welding: fundamentals and applications, Boca Raton, Fla: CRC Press, 2006.

[7] M. Thornton, L. Han and M. Shergold, "Progress in NDT of resistance spot welding of aluminium using ultrasonic C-scan," *NDT & E International,* vol. 48, pp. 30-38, 2012.

[8] K. Benyounis and A. OIabi, "Optimization of different welding processes using statistical and numerical approches - A reference guide," *Advances in Engineering Software,* vol. 39, pp. 483-496, 2008.

[9] L. Lindgren, Computational welding mechanics: thermomechanical and microstructural simulations, Woodhead, 2007.

[10] T. Dupuy, "Estimation of SORPAS results scatter due to numerical parameters," in *6th International Seminar on Advances in Resistance Welding*, Hamburg, 2010.

[11] M. Galler and W. Ernst, "The influence of electrode wear on current density IIW SC 27 09," IIW, 2009.

[12] P. Houldcroft, Feng, Fim and Fweldi, "Welding process developments and future trends," *Materials & Design,* vol. 7, no. 4, pp. 162-169, 1986.

[13] CMW, *Resistance Welding Industries {@ONLINE},* 2012.

[14] G. Solas, J. Sharp and H. Goldsmid, Eds., Thermoelectrics. Basic Principles and New Materials Developments, Springer Heidelberg / New York, 2001.

[15] *ISO 5821:2009 Resistance welding -- Spot welding electrode caps.*

[16] *ISO 5182:2008 Resistance welding -- Materials for electrodes and ancillary equipment.*

[17] A. Rutqvist, An investigation of electrode degradation mechanisms to improve the electrode usage when spot welding, Goteborg: Chalmers tekniska högskola, 2005.

[18] I. Khan, M. Kuntz, L. Zhou, Y. Chan and N. K. Scotchmer, "Monitoring the Effect of RSW Pulsing on AHSS using FEA (SORPAS) Software," vol. 2139, pp. 37-44, 2007.

[19] W. Li, D. Cerjanec and G. A. Grzadzinski, "A comparative study of single-phase AC and multiphase DC resistance spot welding," *Journal of Manufacturing Science and Engineering-Transactions of the Asme,* vol. 127, no. 3, pp. 583-589, 2005.

[20] C. Ma, D. Chen, S. Bhole, G. Boudreau, A. Lee and E. Biro, "Microstructure and fracture characteristics," *Materials Science and Engineering A,* vol. 485, p. 334–346, 2008.

[21] O. Martin, P. D. Tiedra, M. Lopez and M. San-Juan, "Quality prediction of resistance spot welding joints of 304 austenitic stainless steel," *Materials and Design,* vol. 30, pp. 68-77, 2009.

[22] Y. Luo, J. Liu, H. Xu, C. Xiong and L. Liu, "Regression modeling and process analysis of resistance spot welding on galvanized steel sheet," *Materials*

\& *Design,* vol. 30, no. 7, pp. 2547-2555, 2009.

[23] M. Zhou, H. Zhang and S. Hu, "Relationships between Quality and Attributes of Spot Welds," *Welding Journal,* vol. April, pp. 72s - 77s, 2003.

[24] H. Sahai and M. Ageel, The Analysis of Variance: Fixed, Random, and Mixed Models, Birkhäuser, 2000.

[25] G. Archer, "Calculations for temperature response in spot welds," *Welding Journal,* vol. 8, pp. 327s - 330s, 39.

[26] J. Greenwood, "Temperatures in spot welding," *BWRA Report,* pp. 316-322, 1960.

[27] Y. T. and T. Okudo, "A Study of Spot Welding of Heavy Gauge Mild Steel," *Weldíng in the World,* vol. 9, pp. 234-255, 1971.

[28] W. Rice and E. Funk, "An analytical investigation of the temperature distributions during resistance welding," *Welding Journal,* vol. 46, pp. 175s - 186s, 1967.

[29] Z. Han, J. Orozco, J. E. Indacochea and C. H. Chen, "Resistance Spot Welding: A Heat Transfer Study," *Welding Journal,* vol. 68, pp. 363s - 371s, 1989.

[30] H. Cho and Y. Cho, "A study of the thermal behaviour in resistance spot welds," *Welding Journal,* vol. 68, no. 6, pp. 236s-244s, 1989.

[31] J. E. Gould, "Experimental and analytical studies of nugget development during," *Welding Journal,* vol. 66, no. 1, pp. 1s-10s, 1987.

[32] H. Nied, "The Finite Element Modelling of the Resistance Spot Welding Process," *Welding Journal,* vol. 63, pp. 123s-132s, 1984.

[33] N. K. and M. K., "Influence of current wave form on nugget formation phenomena when spot welding thin steel sheet.," *Welding in the World,* vol. 25, pp. 222-244, 1987.

[34] P. S. Wei and C. Y. Ho, "Axisymmetric Nugget Growth During Resistance Spot Welding," *Journal of Heat Transfer,* vol. 112, no. 2, pp. 309-316, 1990.

[35] P. S. Wei and F. B. Yeh, "Factors Affecting Nugget Growth With Mushy-Zone Phase Change During Resistance Spot Welding," *Journal of Heat Transfer,* vol. 113, no. 3, pp. 643-649, 1991.

[36] C. L. Tsai, W. L. Dai, D. W. Dickinson and J. C. Papritan, "ANALYSIS AND DEVELOPMENT OF A REAL-TIME CONTROL METHODOLOGY IN RESISTANCE SPOT-WELDING," *Welding Journal,* vol. 70, no. 12, pp. S339-S351, 1991.

[37] O. P. Gupta and A. De, "An Improved Numerical Modeling for Resistance Spot Welding Process and Its Experimental Verification," *J. Manuf. Sci. Eng.,* vol. 120, pp. 246-252, 1998.

[38] H. Huh and W. Kang, "Electro-thermal analysis of electrode resistance spot welding process by a 3-D finite element method," *Journal of Materials Processing Technology,* vol. 63, p. 672 – 677, 1997.

[39] K. Matsuyama, "Modeling of nugget formation process in resistance spot welding," 1997.

[40] M. Vogler and S. Sheppard, "ELECTRICAL CONTACT RESISTANCE UNDER HIGH LOADS AND ELEVATED-TEMPERATURES," *Welding Journal,* vol. 72, no. 6, pp. S231-S238, 1993.

[41] L. Xu and J. Khan, "Nugget growth model for aluminum alloys during resistance spot welding," *Welding Journal,* vol. 78, p. 367s–372s, 1999.

[42] H. Murakawa, H. Kimura and Y. Ueda, "Weldability analysis of spot welding on aluminum using FEM," *Transactions of JWRI,* vol. 24, p. 101–111, 1995.

[43] E. Feulvarch, P. Rogeon, P. Carr, V. Robin, G. Sibilia and J. Bergheau, "Resistance spot welding process: experimental and numerical modeling of the weld growth mechanisms with consideration of contact conditions," *Numerical Heat Transfer Part A: Applications,* vol. 49, p. 345 – 367, 2006.

[44] SYSWELD Reference Manual, ESI, 2008.

[45] SYSWELD Spot Welding Reference Manual, ESI, 2008.

[46] W. Zhang, "Design and implementation of software for resistance welding process simulations," *Journal of Material and Manufacture,* vol. 112, p. 556–564, 2003.

[47] H. Murakawa, J. Zhang, K. Fujii, J. Wang and M. Ryudo, "FEM Simulation of spot welding process: characteristics of electrode displacement and nugget formation," *Transactions of JWRI,* vol. 29, p. 73–80, 2000.

[48] U. Dilthey and P. Ohse, "The front line in modeling of resistance welding," *Journal of Japan Welding Society,* vol. 76, p. 14–18, 2007.

[49] G. R. Johnson and W. H. Cook, "A constitutive model and data for metals subjected to large strains, high strain rates and high temperatures," 1983.

[50] "MATLAB Documentation," 2007.